Mathematical Modeling in Mechanics of Granular Materials

Mathematical Modelling

Bearbeitet von
Oxana Sadovskaya, Vladimir Sadovskii

1. Auflage 2012. Buch. xii, 392 S. Hardcover
ISBN 978 3 642 29052 7
Format (B x L): 15,5 x 23,5 cm
Gewicht: 765 g

Chapter 2
Rheological Schemes

Abstract The traditional rheological method is supplemented by a new element—rigid contact, which serves to take into account different resistance of a material to tension and compression. A rigid contact describes mechanical properties of an ideal granular material involving rigid particles for an uniaxial stress state. Combining it with elastic, plastic, and viscous elements, one can construct rheological models of different complexity.

2.1 Granular Material With Rigid Particles

The method of rheological models is the basis of the phenomenological approach to the description of a stress-strain state of media with complex mechanical properties, [18, 22, 30]. Ignoring the physical nature of deformation, this method enables one to construct mathematical models which describe quantitative characteristics with a satisfactory accuracy (from the point of view of engineering applications) and are of a good mathematical structure. As a rule, for the models obtained with the help of the rheological method, solvability of main boundary-value problems can be analyzed and efficient algorithms for numerical implementation can be easily constructed. At the same time, with the use of conventional rheological elements (a spring simulating elastic properties of a material, a viscous damper, and a plastic hinge) only, it is impossible to construct a rheological scheme for a medium with different resistance to tension and compression or for a medium with different ultimate strengths under tension and compression.

To make it possible, we supplement the method by a new, fourth element, namely, a rigid contact, [26–28]. It is represented schematically as two plates being in contact (Fig. 2.1). A granular material with rigid particles, i.e. a system of absolutely rigid balls being in contact with each other, is an ideal material whose behavior at a uniaxial stress-strain state corresponds to this element. With tension of a system, balls roll about and stress turns out to be zero. Following previous tension, compression goes

O. Sadovskaya and V. Sadovskii, *Mathematical Modeling in Mechanics of Granular Materials*, Advanced Structured Materials 21,
DOI: 10.1007/978-3-642-29053-4_2,

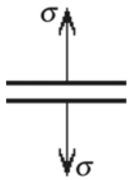

Fig. 2.1 Rigid contact element

on with zero stresses until the balls touch each other and the system in fact returns to its original position. Compressive strains are impermissible and compressive stresses can be arbitrary with strain being equal to zero.

With the conventional notations, we represent the constitutive relationships of a rigid contact as the system

$$\sigma \leq 0, \quad \varepsilon \geq 0, \quad \sigma\,\varepsilon = 0. \tag{2.1}$$

The inequalities involved in this system exclude arising tensile stresses and compressive strains in a granular material with rigid particles. From the equation (so-called complementing condition) it follows that one of the quantities being considered (stress or strain) must be zero.

It should be noted that the constitutive relationships (2.1) are incorrect in the mechanical sense because in the general case they do not enable one to determine uniquely acting stress from given strain and, conversely, to determine strain from given stress. However, as will be shown further, this incorrectness can be easily eliminated by adding regularizing elements to the rheological scheme.

Similar systems of inequalities with complementing conditions arise, for example, in mathematical economics when solving problems of multiple objective optimization (see, [8, 23]). It is known that such a system can be reduced to two variational inequalities equivalent to one another (arbitrary varying quantities are marked by tilde):

$$\sigma\,(\tilde{\varepsilon} - \varepsilon) \leq 0, \quad \varepsilon, \tilde{\varepsilon} \geq 0; \quad (\tilde{\sigma} - \sigma)\,\varepsilon \leq 0, \quad \sigma, \tilde{\sigma} \leq 0. \tag{2.2}$$

Indeed, let the system (2.1) be valid for σ and ε. Then either $\sigma = 0$ and $\varepsilon \geq 0$, or $\sigma < 0$ and $\varepsilon = 0$. In either case both inequalities (2.2) hold since, on the one hand, $\sigma\,\tilde{\varepsilon} \leq 0$ and, on the other hand, $\tilde{\sigma}\,\varepsilon \leq 0$. Now assume that on the contrary σ and ε satisfy the first inequality of (2.2). Then either $\varepsilon = 0$ and the relationships (2.1) are evident, or $\varepsilon > 0$ and from the fact that strain variation may be positive ($\tilde{\varepsilon} > \varepsilon$) as well as negative ($\varepsilon > \tilde{\varepsilon} \geq 0$) it follows that σ equals zero. In this case the relationships (2.1) are also evident. If σ and ε satisfy the second inequality of (2.2) rather than the first one, then the system (2.1) is valid for them. This is proved in a similar way.

The advantage of the formulation of constitutive relationships of a rigid contact in terms of variational inequalities over the equivalent formulation (2.1) lies in the fact that these inequalities admit a generalization to the case of a spatial stress-strain state of a medium. This generalization is given in Chap. 4. It is performed with the help

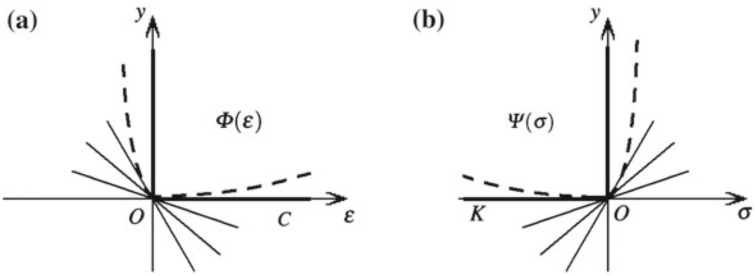

Fig. 2.2 Stress potential **a** and strain potential **b**

of tensor representations by introducing cones of admissible strains and stresses. In the uniaxial state considered now these cones are equal to $C = \{\varepsilon \geq 0\}$ and $K = \{\sigma \leq 0\}$, respectively. To state the potential nature of the relationships, we represent (2.2) in the following form:

$$\sigma \in \partial\Phi(\varepsilon), \quad \varepsilon \in \partial\Psi(\sigma). \tag{2.3}$$

Here Φ and Ψ are the stress and strain potentials, the symbol ∂ denotes subdifferential.

Contrary to the classical models of mechanics of deformable media, in this case the potentials are not differentiable and even continuous. They are defined in terms of the indicator functions of the cones C and K:

$$\Phi(\varepsilon) = \begin{cases} 0, & \text{if } \varepsilon \in C, \\ +\infty, & \text{if } \varepsilon \notin C, \end{cases} \quad \Psi(\sigma) = \begin{cases} 0, & \text{if } \sigma \in K, \\ +\infty, & \text{if } \sigma \notin K, \end{cases}$$

for which the conventional notations $\delta_C(\varepsilon)$ and $\delta_K(\sigma)$ are used further. The graph of the former function is formed by two positive semi-axes on the $\varepsilon\, y$ plane and the graph of the latter one by negative and positive semi-axes on the $\sigma\, y$ plane (Fig. 2.2). Both of them can be obtained by passage to the limit with the help of sequences of continuously differentiable functions whose graphs are shown as dashed lines. Smoothed functions can be considered as potentials of special nonlinearly elastic media with different strength properties to tension and compression. For such media the nonlinear Hooke law is valid: stresses are expressed in terms of derivatives with respect to strains and vice versa. In the limit the derivatives, with which the angular coefficients of tangents to graphs of smooth potentials are identified, are transformed to subdifferentials of the indicator functions. For the interior points of the cones C and K they tend to zero and for the boundary points ($\varepsilon = 0$ and $\sigma = 0$, respectively) they may take any limit position shown in Fig. 2.2 as a fan of straight lines.

A rigorous mathematical definition of subdifferential of a convex function and some its properties required for the study of models of spatial deformation of a granular material are given in Chap. 3. Here, basing on the intuitive notion described above, we only state that subdifferential of a function at a given point is the set formed by angular coefficients of all straight lines, "tangent" to the graph of the function at this point and lying below the graph. Thus, if $\varepsilon \in C$ and $\sigma \in K$ then

$$\partial\delta_C(\varepsilon) = \left\{\tilde{\sigma} \;\middle|\; \tilde{\sigma}\,(\tilde{\varepsilon} - \varepsilon) \le 0 \;\; \forall\, \tilde{\varepsilon} \ge 0\right\},$$

$$\partial\delta_K(\sigma) = \left\{\tilde{\varepsilon} \;\middle|\; (\tilde{\sigma} - \sigma)\,\tilde{\varepsilon} \le 0 \;\; \forall\, \tilde{\sigma} \le 0\right\},$$

and going from Eq. (2.2) to (2.3) is a trivial change of notations for a more illustrative geometric interpretation. We also note that it makes no sense to look for a form of phenomenological constitutive relationships for an ideal granular material with rigid particles which is more simple than (2.3) since the notions and notations being used describe a threshold nature of deformation of a material with extreme precision. Besides, they are a simple generalization of the constitutive equations of the nonlinear elasticity theory to the case of non-differentiable potentials.

2.2 Elastic-Visco-Plastic Materials

A known way of regularization of incorrect mechanical model is in going to a more complex model describing adequately special features of deformation of a material which are not taken into account. As a version of complication, we consider the model of an ideal granular material with elastic particles whose rheological scheme is given in Fig. 2.3a. According to this scheme, strain is equal to the sum of an elastic component $\varepsilon^e = a\,\sigma$ (computed by the Hooke law), where $a > 0$ is the modulus of elastic compliance of a spring, and strain $\varepsilon^c = \varepsilon - \varepsilon^e$ of a rigid contact. If $\sigma < 0$ then $\varepsilon^c = 0$ and $\varepsilon = a\,\sigma < 0$, i.e. elastic compression takes place. If $\sigma = 0$ then $\varepsilon^e = 0$ and $\varepsilon \ge 0$, i.e. the loosening of a material is observed. In the general case the real stress is determined in terms of the strain by the formula

$$\sigma = \frac{\varepsilon - |\varepsilon|}{2\,a}. \tag{2.4}$$

On the contrary, generally speaking, the strain is not uniquely determined in terms of given stress. Thus, the model of an elastic granular material is as much incorrect as the model of an elastic-plastic material with hardening being not taken into account, [9]. The constitutive relationships can be represented in the potential form (2.3) with potentials

$$\Phi(\varepsilon) = \begin{cases} \varepsilon^2/(2\,a), & \text{if } \varepsilon < 0, \\ 0, & \text{if } \varepsilon \ge 0, \end{cases} \qquad \Psi(\sigma) = \frac{a\,\sigma^2}{2} + \delta_K(\sigma).$$

The former potential is a differentiable function and the latter one takes infinite values exterior to the cone K. This expression for the stress potential is obtained as a solution of the differential equation $\partial\Phi/\partial\varepsilon = \sigma$ with the right-hand side (2.4), and

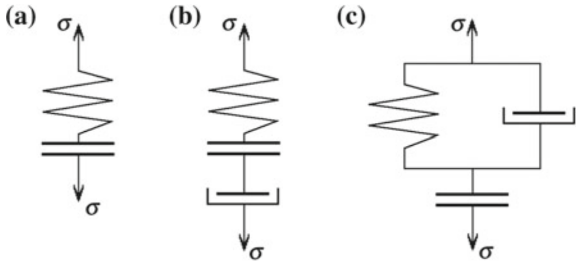

Fig. 2.3 Rheological schemes: **a** elastic granular material, **b** viscoelastic material (Maxwell model), **c** viscoelastic material (Kelvin–Voigt model)

for the strain potential it is obtained as a consequence of an additive representation in the form of the sum of potentials of an elastic spring and a rigid contact.

The rheological schemes shown in Figs. 2.3b,c correspond to granular materials which show viscoelastic properties in the compression process. In both cases, ideal (cohesionless) materials are considered. The scheme in Fig. 2.3b describes compression with the help of the Maxwell model and the scheme in Fig. 2.3c with the help of the Kelvin–Voigt model. For the former scheme from Eq. (2.4), taking into account the Newton law $\sigma = \eta\,\dot{\varepsilon}^v$, we have

$$2\,a\,\eta\,\dot{\varepsilon}^v = \varepsilon - \varepsilon^v - |\varepsilon - \varepsilon^v| \le 0. \tag{2.5}$$

Here η is the viscosity coefficient and $\dot{\varepsilon}^v$ is the rate of the viscous strain. If the time-dependence of stress $\sigma(t) \le 0$ is known, then the viscous strain component is determined by integration of the equation corresponding to the Newton law. To determine total deformation, Eq. (2.5) whose solution is, in general, ambiguous is used. When, on the contrary, the dependence $\varepsilon(t)$ is given, then, integrating the differential Eq. (2.5), we can determine the dependence $\varepsilon^v(t)$ and, hence, $\sigma(t)$.

The solution of the differential equation is conveniently interpreted geometrically on the $\varepsilon\,\varepsilon^v$ plane. For $\varepsilon \ge \varepsilon^v$ the rate of viscous strain equals zero and for $\varepsilon < \varepsilon^v$ the equation $a\,\eta\,\dot{\varepsilon}^v = \varepsilon - \varepsilon^v$ holds. Hence,

$$\varepsilon^v = \varepsilon_0^v \exp\Big(-\frac{t - t_0}{a\,\eta}\Big) + \frac{1}{a\,\eta}\int_{t_0}^{t} \varepsilon(t_1)\exp\Big(-\frac{t - t_1}{a\,\eta}\Big)dt_1,$$

where ε_0^v and t_0 are constants. In Fig. 2.4 the typical deformation curve is shown. The ray $O\,P_0$ corresponds to tension of a material for $\varepsilon_0^v = 0$ and the curve $O\,P_1\,P_2$ depending on $\varepsilon(t)$ corresponds to compression. At the point P_1 the strain rate changes its sign from negative to positive. At the point P_2 an irreversibly compressed material transforms to a loosened state. In the case of slow (quasistatic) compression, the curve $O\,P_1\,P_2$ tends to the rectilinear segment $O\,P_2$ of the ray $\varepsilon = \varepsilon^v \le 0$ shown as a dashed line. When repeating a deformation cycle, a similar curve issues out of the point P_2 rather than of O.

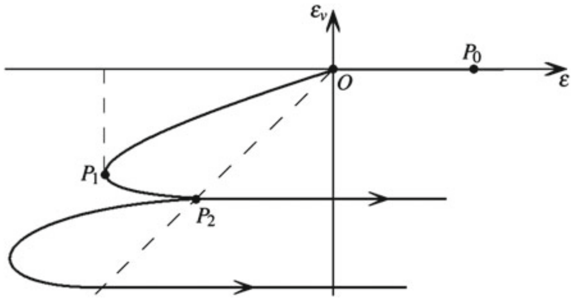

Fig. 2.4 Deformation curve (Maxwell model)

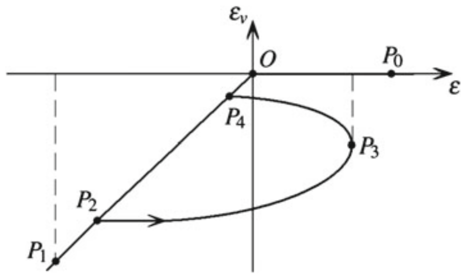

Fig. 2.5 Deformation curve (Kelvin–Voigt model)

For the latter scheme, stress consists of two components (elastic and viscous) $\sigma = \sigma^e + \sigma^v$ and strains of viscous and elastic elements coincide. Thus,

$$\varepsilon = \varepsilon^c + \varepsilon^v, \quad \sigma = \frac{\varepsilon^v}{a} + \eta\,\dot{\varepsilon}^v. \tag{2.6}$$

For $\varepsilon^c > 0$, when a material is loosened, stress equals zero, hence,

$$\varepsilon^v = \varepsilon_0^v \exp\Bigl(-\frac{t - t_0}{a\,\eta}\Bigr). \tag{2.7}$$

For $\varepsilon^c = 0$, when a material is in a compact state, stress $\sigma \le 0$ is calculated from given strain by Eq. (2.6) for $\varepsilon^v = \varepsilon$. The typical deformation curve for given dependence $\varepsilon(t)$ is shown in Fig. 2.5. Tension is described by the ray OP_0 and compression by the rectilinear segment OP_1. At the point P_1 the strain rate $\dot{\varepsilon}$ changes sign. In the segment P_1P_2 unloading is performed for $\varepsilon^c = 0$ and $\sigma < 0$. The viscoelastic component of strain relaxes. Stress turns out to be equal to zero at some point P_2 and the further process is consistent with Eq. (2.7). The curve $P_2P_3P_4$ is associated with this equation. At the point P_4 a cycle of repeated deformation starts.

Total strain is uniquely determined from a given dependence $\sigma(t) \le 0$ only in a viscoelastic compression state for $\varepsilon^c = 0$,

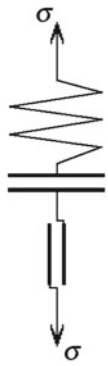

Fig. 2.6 Rheological scheme with plastic element

$$\varepsilon^v = \varepsilon_0^v \exp\Bigl(-\frac{t-t_0}{a\,\eta}\Bigr) + \frac{1}{\eta}\int\limits_{t_0}^{t} \sigma(t_1)\exp\Bigl(-\frac{t-t_1}{a\,\eta}\Bigr)dt_1.$$

In a tension state the model remains incorrect due to ambiguity of strain of a contact.

The rheological scheme of an ideal elastic-plastic granular material is shown in Fig. 2.6. With tension or compression under the action of stress whose absolute value does not exceed the yield point σ_s of a plastic hinge, such a material behaves according to the scheme shown in Fig. 2.3a. As the yield point is achieved, with compression the material passes to a plastic flow state. In this state, the strain rate $\dot{\varepsilon}$ can take an arbitrary negative value. If, following a plastic flow state, stress decreases (unloading occurs) but remains compressing, then the strain rate is expressed in terms of the stress rate by the linear Hooke law. Stresses exceeding σ_s are impermissible.

Total strain involves three components associated with three elements of the scheme: $\varepsilon = \varepsilon^e + \varepsilon^c + \varepsilon^p$. Due to (2.4)

$$2\,a\,\sigma = \varepsilon - \varepsilon^p - |\varepsilon - \varepsilon^p| \le 0.$$

Taking into account the sign of stress, we write the constitutive relationships of a plastic hinge as a system of inequalities with the complementing condition

$$\dot{\varepsilon}^p \le 0, \quad \sigma \ge -\sigma_s, \quad (\sigma + \sigma_s)\,\dot{\varepsilon}^p = 0.$$

Similarly to (2.1), this system can be transformed to equivalent variational inequalities or reduced to the potential form. To this end, we first consider the potential representation of the Newton law for a viscous flow:

$$\sigma = \frac{\partial D(\dot{\varepsilon}^v)}{\partial \dot{\varepsilon}^v}, \quad \dot{\varepsilon}^v = \frac{\partial H(\sigma)}{\partial \sigma}.$$

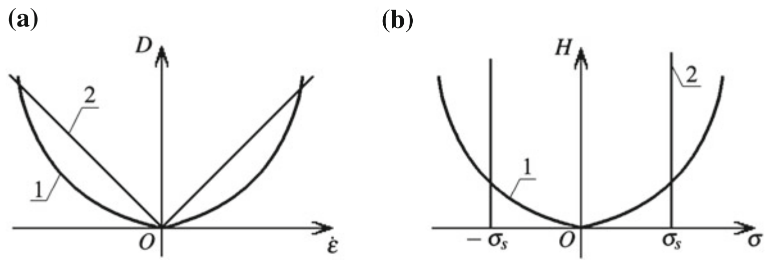

Fig. 2.7 Dissipative potentials of stresses **a** and strain rates **b**

If the coefficient of viscosity is constant, the dissipative potentials $D = \eta\,(\dot{\varepsilon}^v)^2/2$ and $H = \sigma^2/(2\,\eta)$ are quadratic functions (curves 1 in Fig. 2.7). Deforming the graphs with preservation of convexity, we can obtain potentials for a material with a variable viscosity coefficient depending on achieved stress or instant strain rate. To retain consistency of potentials, the graphs D and H should be deformed so that these functions are expressed in terms of one another with the help of the Legendre tangent transform

$$H(\sigma) = \sigma\,\dot{\varepsilon}^v - D(\dot{\varepsilon}^v).$$

Convexity is required for a viscosity coefficient to be positive. The limit version of convex curves (the piecewise linear curves 2) corresponds to the plastic state of a material. The existence of corner points on graphs of plastic dissipative potentials leads to the necessity of using subdifferential which generalizes the notion of derivative. The constitutive relationships $\sigma \in \partial D(\dot{\varepsilon}^p)$ and $\dot{\varepsilon}^p \in \partial H(\sigma)$ in terms of subdifferentials result in two inequalities

$$\sigma\,(\tilde{e} - \dot{\varepsilon}^p) \leq D(\tilde{e}) - D(\dot{\varepsilon}^p) \quad \forall\, \tilde{e},$$

$$(\tilde{\sigma} - \sigma)\,\dot{\varepsilon}^p \leq 0, \quad |\sigma| \leq \sigma_s, \quad |\tilde{\sigma}| \leq \sigma_s.$$

Their equivalence can be proved on the basis of the results given in the next chapter.

For an elastic-plastic granular material (Fig. 2.6), this leads to the variational inequality

$$(\tilde{\sigma} - \sigma)(a\,\dot{\sigma} - \dot{\varepsilon}) \geq 0, \quad |\sigma| \leq \sigma_s, \quad |\tilde{\sigma}| \leq \sigma_s, \tag{2.8}$$

which provides an exact description of rheology of a plastic element. Consider the $\sigma - \varepsilon$ diagrams of the uniaxial deformation for such a material (Fig. 2.8) constructed with the help of (2.8). The $\sigma - \varepsilon$ diagram shows the active loading as a three-segment broken line whose segments correspond to the loosening of a material (the segment $O P_0$) and to the elastic and plastic compression ($O P_1$ and $P_1 P_2$, respectively). The unloading following the plastic flow of a material is described as the rectilinear segment $P_2 P_3$ which is parallel to the original elastic segment of the diagram.

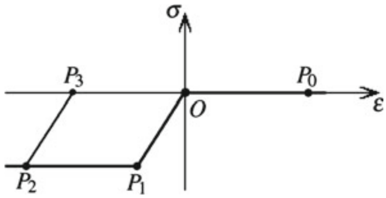

Fig. 2.8 Diagram of uniaxial tension–compression

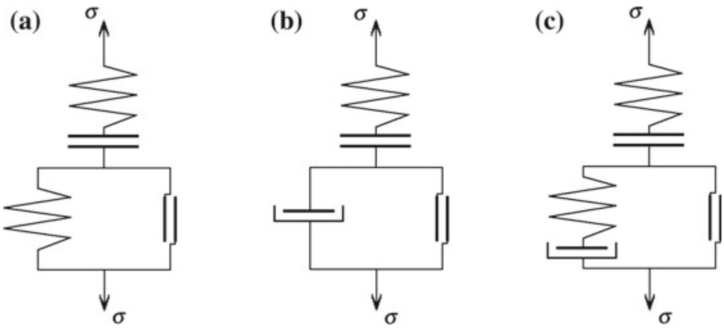

Fig. 2.9 Complex rheological schemes: **a** elastic-plastic granular material, **b** elastic-visco-plastic granular material (Schwedoff–Bingham model), **c** regularized variant of previous scheme

Combining elastic, plastic and viscous elements with a rigid contact, we can construct constitutive relationships for granular materials of more complex rheology. Examples of more complex schemes are given in Fig. 2.9. The scheme in Fig. 2.9a describes a granular material whose deformation with compressive stresses is defined by the theory of elastic-plastic flow with linear hardening. The schemes in Figs. 2.9b,c correspond to the theory of viscoplastic Schwedoff–Bingham flow.

In conclusion, it should be noted that a rigid contact, using in the given approach to take into account different compression and tension strength properties of the granular material and being in fact a nonlinearly elastic element, describes a thermodynamically reversible process. Irreversible deformation of a material which results in dissipation of mechanical energy is taken into account only when viscous or plastic elements are involved into the rheological scheme.

2.3 Cohesive Granular Materials

Further development of the model of a granular material leading to constitutive relationships correct in the mechanical sense consists in the phenomenological description of connections between particles. To this end, in parallel with a rigid contact, an elastic, viscous, or plastic element is involved into a scheme depending on properties of the binder. The simplest rheological scheme taking into account elastic connections between absolutely rigid particles is given in Fig. 2.10a. Figure 2.10b

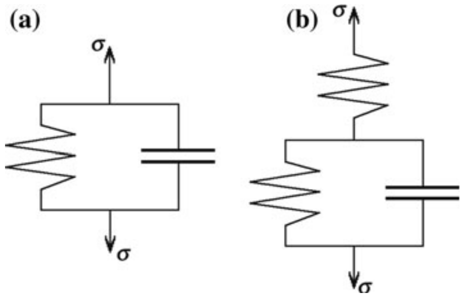

Fig. 2.10 Elastic connections: **a** elastic material with rigid particles, **b** heteromodular elastic material

corresponds to a model of a heteromodular elastic material whose elastic properties with tension are characterized by two series-connected springs and with compression by only one of these springs. In this case the constitutive equations

$$\varepsilon = \begin{cases} (a+b)\,\sigma, & \text{if } \sigma \geq 0, \\ a\,\sigma, & \text{if } \sigma < 0, \end{cases}$$

(a and b are the moduli of elastic compliance) describe a one-to-one dependence between stress and strain.

Viscous properties of a binder are taken into account in the rheological schemes in Fig. 2.11. The scheme given in Fig. 2.11a serves to describe a cohesive granular material with absolutely rigid particles. In the scheme shown in Fig. 2.11b particles with compression are deformed according to the elastic law. More complicated rheology can be taken into account with the help of the models considered in the above section. According to the second scheme, for $\varepsilon^c = \varepsilon - a\,\sigma > 0$ the strain of the material obeys the Maxwell model. If the dependence $\sigma(t)$ is given, the unknown time-dependence of strain is uniquely determined by integrating the equation

$$\dot{\varepsilon} = a\,\dot{\sigma} + \frac{\sigma}{\eta}, \tag{2.9}$$

whose solution describes a real process provided that $\varepsilon \geq a\,\sigma$. With violating this condition, strain is determined from the Hooke law as $\varepsilon = a\,\sigma$. If the dependence $\varepsilon(t)$ is given, then the function $\sigma(t)$ describing the stress state of a material with the same condition is determined by integrating Eq. (2.9). Otherwise real stress is determined from the Hooke law. Thus, the model is correct for an arbitrary program of deformation or loading.

In Fig. 2.12a the rheological scheme of a material involving rigid particles with plastic connections is given. Deformation of such a material is possible provided that the absolute value of stress is equal to the yield point of a plastic hinge. Compression is admissible only after previous tension. Any deformation is thermodynamically irreversible. The rheological scheme given in Fig. 2.12b takes into account, along with plastic properties of a binder, its elastic properties and elastic properties of

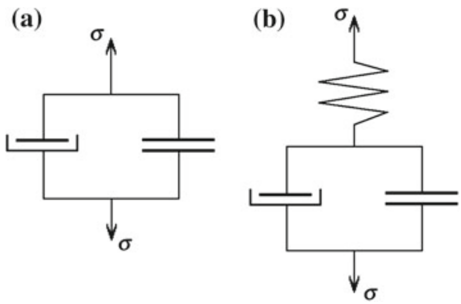

Fig. 2.11 Viscous connections: **a** cohesive material with rigid particles, **b** viscoelastic granular material

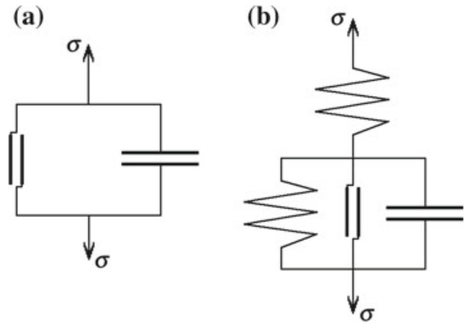

Fig. 2.12 Plastic connections: **a** plastic material with rigid particles, **b** elastic-plastic granular material

particles. This model is quite correct since the corresponding diagram of uniaxial tension–compression (Fig. 2.13) is strictly monotone on the active loading segments OP_0 and OP_1P_2 as well as on the unloading segment $P_2P_3P_4$. On the segments OP_0 and OP_1 elastic deformation of a material is observed. The segment P_1P_2 of the diagram describes the process of plastic tension of natural (no hardening) material. In this case

$$\varepsilon = a\,\sigma + b\,(\sigma - \sigma_s).$$

On the elastic unloading segment P_2P_3 strain of the upper spring is equal to $a\,\sigma$ and the strain of the system of parallel elements is constant:

$$\varepsilon^e = \varepsilon^p = \text{const}, \quad \sigma^e = \frac{\varepsilon^p}{b}, \quad \sigma^p = \sigma - \sigma^e.$$

At the point P_3 stress of a plastic hinge achieves the yield point $(-\sigma_s)$ with compression and a material is transformed into a state of plastic flow (the segment P_3P_4) described by the equation

$$\varepsilon = a\,\sigma + b\,(\sigma + \sigma_s).$$

At the point P_4 symmetric to P_1 contact is closed up, i.e. its strain $\varepsilon^c = b\,(\sigma + \sigma_s)$ turned out to be zero. Thus, in the framework of the model with the rheological scheme given in Fig. 2.12b, with the cyclic loading, the translational strain hardening of the

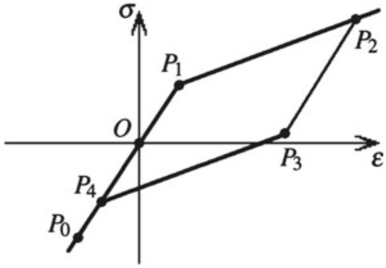

Fig. 2.13 Diagram of uniaxial tension–compression

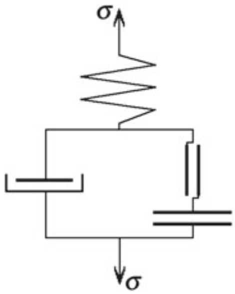

Fig. 2.14 Scheme involving four different elements

material is observed. However, as the cycle is completed, the yield surface takes its original position.

More complex rheological properties of particles and the binder are taken into account in the scheme involving four elements of different types shown in Fig. 2.14. This is probably the only version of the configuration of four elements which results in a model correct in the mechanical sense. Judging by this scheme, in the tension state, where $\varepsilon^c = \varepsilon^v - \varepsilon^p > 0$, a plastic hinge has no effect, hence, behavior of a material is described by the Maxwell model of a viscoelastic medium. In the compression state, where a contact is closed up, a material behaves as the Schwedoff–Bingham elastic-visco-plastic medium. The equations

$$\sigma = \sigma^e = \sigma^v, \quad \varepsilon = \varepsilon^e + \varepsilon^v, \quad \varepsilon^e = a\,\sigma, \quad \eta\,\dot{\varepsilon}^v = \sigma$$

form a total system for determining strain from given stress or stress from given strain for $\varepsilon^v > \varepsilon^p$. Hence it follows that strain is determined in terms of stress by integrating the differential equation (2.9) with respect to ε and stress is determined in terms of strain with the help of the same equation with respect to σ. In this case the general solution is given by the integral

$$\sigma = s(t) \equiv \sigma_0 \exp\Bigl(-\frac{t - t_0}{a\,\eta}\Bigr) + \frac{1}{a}\int_{t_0}^{t} \exp\Bigl(-\frac{t - t_1}{a\,\eta}\Bigr) \mathrm{d}\varepsilon(t_1), \tag{2.10}$$

where the integration constant σ_0 is determined from the condition for continuity of stress with change of mode, t_0 is the instant of going to a given mode. Thus, all unknown functions turn out to be uniquely determined.

With compression, different variants may take place. If compression follows previous tension of a material and, hence, $\varepsilon^c > 0$, then the process is described by Eqs. (2.9), (2.10) up to the instant at which a contact is closed up. For $\varepsilon^c = 0$ the equations

$$\sigma = \sigma^e = \sigma^v + \sigma^c, \quad \sigma^c = \sigma^p, \quad \varepsilon = \varepsilon^e + \varepsilon^v, \quad \varepsilon^v = \varepsilon^p$$

are valid. For $0 > \sigma > -\sigma_s$ a plastic element blocks deformation of a viscous damper and viscous stress σ^v turns out to be zero. In this state a material is deformed according to the Hooke law $\varepsilon = a\,\sigma$. Finally, for $\sigma \leq -\sigma_s$ the equality $\sigma^p = -\sigma_s$ holds, hence,

$$\dot{\varepsilon} = a\,\dot{\sigma} + \frac{\sigma + \sigma_s}{\eta}, \quad \sigma = s(t) - \sigma_s. \tag{2.11}$$

All unknown functions are also uniquely determined.

If a loading or deformation program involves alternating tension and compression segments then the unknown time-dependences of strain and stress, respectively, can be obtained in a closed form with the help of Eqs. (2.9), (2.10), and (2.11). Only a choice of an appropriate mode presents difficulties. To give a rigorous mathematical formulation of the problem in the general case (for arbitrary loading and deformation programs) which allows one to solve the problem of choice implicitly, we supplement the equations with universal constitutive relationships for a rigid contact and a plastic hinge in the form of variational inequalities (2.2) and (2.8):

$$\sigma^c\,(\tilde{\varepsilon} - \varepsilon^c) \leq 0, \quad \varepsilon^c \geq 0, \ \ \tilde{\varepsilon} \geq 0,$$

$$(\tilde{\sigma} - \sigma^p)\,\dot{\varepsilon}^p \leq 0, \quad |\sigma^p| \leq \sigma_s, \ \ |\tilde{\sigma}| \leq \sigma_s,$$

which involve arbitrary admissible variations of stress and strain. Besides, we formulate initial conditions for viscous and plastic elements for which the constitutive relationships are of the differential form: $\varepsilon^v(0) = \varepsilon^p(0) = 0$.

2.4 Computer Modeling

The construction and study of constitutive relationships for materials whose rheological schemes involve a reasonably large number of elements are rather tedious. In this section, a way of the solution of this problem with the use of general-purpose computational algorithms implemented in the form of a computer system with elements of visual design, [31], is proposed.

In the general case the analysis of rheological properties of materials with uniaxial deformation is reduced to two problems considered above. In the first problem a loading program (the time-dependence of stress σ) is known and the time-dependence of strain $\varepsilon(t)$ is unknown. In the second one, conversely, a deformation program is given and the time-dependence of stress is to be determined. In the case of constant tensile or compressive stress, the solution of the first problem enables one to construct the creep diagrams of a material. The second problem provides curves of the stress relaxation in the case of constant strain.

If the scheme of a material being studied involves nonlinear elements (plastic hinges or rigid contacts) then in a natural way the question of correctness of a rheological model arises. A model is assumed to be correct if both problems are uniquely solvable and stable. For example, the model of ideal plasticity whose rheological scheme involves a single element, namely, a plastic hinge, is among incorrect models. For given stress being equal to the yield point, strain can not be uniquely determined in the framework of this model. The model of an ideal granular material with absolutely rigid particles, whose rheological scheme is represented by a rigid contact (Fig. 2.1), is another example of an incorrect model. In this case, for $\sigma = 0$ strain is not uniquely determined, besides, stress is not uniquely determined for $\varepsilon = 0$.

Among correct models, further we consider only the models which enable us to determine stresses and strains of all elements of a rheological scheme. Most likely it is difficult to formulate in the general case the conditions under which a model has this property. Because of this, further this question is related to correctness of a computational algorithm being applied. An example of a rheological scheme involving four base elements of different types which is correct in this sense is given in Fig. 2.14 of the previous section.

In the general case a rheological scheme involving n elements is subdivided into m levels depending on the position of connective elements. Each level is characterized by strain ε_i, $i = 1, \ldots, m$. Elements are numbered in a strictly specified order: first elastic elements, next viscous ones, then rigid contacts, and finally plastic hinges. To each of them, there corresponds stress σ_j, $j = 1, \ldots, n$. Let $\boldsymbol{U}$ be a vector of dimension $N = m + n + 1$ such that these $m + n$ quantities and one more quantity (the unknown value of total strain or of resulting stress, according to the type of a problem) are its components. A rheological scheme of the general form leads to a system involving algebraic equations (equilibrium conditions and constitutive equations for elastic elements)

$$\sum_{j=1}^{N} a_{ij}\, U_j = f_i(t), \quad i = 1, \ldots, N_1, \tag{2.12}$$

ordinary differential equations specifying viscous elements

$$\sum_{j=1}^{N} a_{ij}\, \dot{U}_j = U_i, \quad i = N_1 + 1, \ldots, N_2, \tag{2.13}$$

and variational inequalities for rigid contacts

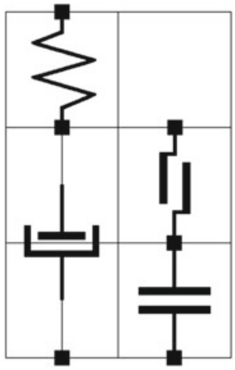

Fig. 2.15 Graphical representation of a scheme

$$(\tilde{V}_i - V_i)\, U_i \le 0, \quad V_i \equiv \sum_{j=1}^{N} a_{ij}\, U_j \ge 0, \quad \tilde{V}_i \ge 0, \quad i = N_2 + 1, \ldots, N_3, \quad (2.14)$$

and for plastic hinges

$$(\tilde{U}_i - U_i) \sum_{j=1}^{N} a_{ij}\, \dot{U}_j \le 0, \quad |U_i| \le U_i^*, \quad |\tilde{U}_i| \le U_i^*, \quad i = N_3 + 1, \ldots, N, \quad (2.15)$$

with the initial conditions

$$\sum_{j=1}^{N} a_{ij}\, U_j(0) = 0, \quad i = N_1 + 1, \ldots, N_2, N_3 + 1, \ldots, N.$$

The coefficients a_{ij} involved in the system (2.12)–(2.15) may be equal to 0, ± 1 or take the values of the moduli of elasticity and the viscosity coefficients.

For example, the rheological scheme shown in Fig. 2.14 has three levels ($m = 3$, $n = 4$) whose boundaries pass through the nodes of connections (see Fig. 2.15). Strains of elements are determined by the formulae $\varepsilon^e = \varepsilon_1$, $\varepsilon^v = \varepsilon_2 + \varepsilon_3$, $\varepsilon^p = \varepsilon_2$, $\varepsilon^c = \varepsilon_3$. The elements are numbered in the following order: elastic (e), viscous (v), a rigid contact (c), and a plastic hinge (p). For this scheme $N_1 = 5$, $N_2 = 6$, $N_3 = 7$, $N = 8$. In the first problem a vector of unknown functions is represented in the form $\boldsymbol{U} = (\varepsilon, \varepsilon_1, \varepsilon_2, \varepsilon_3, \sigma_1, \sigma_2, \sigma_3, \sigma_4)$. In the second problem, in place of total strain $\varepsilon = \varepsilon^e + \varepsilon^v$, stress $\sigma = \sigma^e = \sigma_1$ is repeated in this vector. Rectangular matrix $\mathsf{A} \sim a_{ij}$ and vector $\boldsymbol{F} \sim f_i$ can be composed of the coefficients of the equations and inequalities. For the first problem

$$\mathsf{A} = \begin{pmatrix} -1 & 1 & 1 & 1 & 0 & 0 & 0 & 0 \\ 0 & 0 & 0 & 0 & 1 & 0 & 0 & 0 \\ 0 & 0 & 0 & 0 & -1 & 1 & 0 & 1 \\ 0 & 0 & 0 & 0 & 0 & 0 & 1 & -1 \\ 0 & -1 & 0 & 0 & a & 0 & 0 & 0 \\ 0 & 0 & \eta & \eta & 0 & 0 & 0 & 0 \\ 0 & 0 & 0 & 1 & 0 & 0 & 0 & 0 \\ 0 & 0 & 1 & 0 & 0 & 0 & 0 & 0 \end{pmatrix}, \quad \boldsymbol{F} = \begin{pmatrix} 0 \\ \sigma(t) \\ 0 \\ 0 \\ 0 \end{pmatrix}.$$

For the second problem

$$\mathsf{A} = \begin{pmatrix} 0 & 1 & 1 & 1 & 0 & 0 & 0 & 0 \\ -1 & 0 & 0 & 0 & 1 & 0 & 0 & 0 \\ 0 & 0 & 0 & 0 & -1 & 1 & 0 & 1 \\ 0 & 0 & 0 & 0 & 0 & 0 & 1 & -1 \\ 0 & -1 & 0 & 0 & a & 0 & 0 & 0 \\ 0 & 0 & \eta & \eta & 0 & 0 & 0 & 0 \\ 0 & 0 & 0 & 1 & 0 & 0 & 0 & 0 \\ 0 & 0 & 1 & 0 & 0 & 0 & 0 & 0 \end{pmatrix}, \quad \boldsymbol{F} = \begin{pmatrix} \varepsilon(t) \\ 0 \\ 0 \\ 0 \\ 0 \end{pmatrix}.$$

It is evident that a rheological scheme of any level of complexity can be described with the help of the system (2.12)–(2.15). Approximation of the derivatives involved in this system leads to the equations and inequalities

$$\sum_{j=1}^{N} a_{ij}\, U_j^{k+1} = f_i^{k+1}, \quad \sum_{j=1}^{N} a_{ij}\big(U_j^{k+1} - U_j^k\big) = \Delta t\; U_i^{k+1}, \tag{2.16}$$

$$\big(\tilde{V}_i - V_i^{k+1}\big)\, U_i^{k+1} \le 0, \quad V_i^{k+1} = \sum_{j=1}^{N} a_{ij}\, U_j^{k+1} \ge 0, \quad \tilde{V}_i \ge 0, \tag{2.17}$$

$$\big(\tilde{U}_i - U_i^{k+1}\big) \sum_{j=1}^{N} a_{ij}\big(U_j^{k+1} - U_j^k\big) \le 0, \quad \big|U_i^{k+1}\big| \le U_i^*, \quad |\tilde{U}_i| \le U_i^*. \tag{2.18}$$

The limits of variation of subscript i which are given in the corresponding formulae (2.12)–(2.15) are omitted here for brevity.

Repeating the reasoning, given in Sect. 2.1 when justifying the formulation of constitutive relationships for a rigid contact in the form of the variational inequalities (2.2), it is easy to show that the inequality (2.17) is equivalent to the alternative: either $V_i^{k+1} = 0$ and at the same time $U_i^{k+1} \le 0$ or $V_i^{k+1} > 0$ and $U_i^{k+1} = 0$. In a similar way, the inequality (2.18) is reduced to the choice of one of three alternatives:

$$\text{(i)}\quad \left|U_i^{k+1}\right| < U_i^*, \quad \sum_{j=1}^{N} a_{ij}\left(U_j^{k+1} - U_j^k\right) = 0,$$

$$\text{(ii)}\quad U_i^{k+1} = U_i^*, \quad \sum_{j=1}^{N} a_{ij}\left(U_j^{k+1} - U_j^k\right) \geq 0,$$

$$\text{(iii)}\quad U_i^{k+1} = -U_i^*, \quad \sum_{j=1}^{N} a_{ij}\left(U_j^{k+1} - U_j^k\right) \leq 0.$$

For the first variant, stress of a plastic hinge is lower than the limit level, hence, the plastic strain rate equals zero. For the second variant, on tension the stress coincides with the yield point, hence, the strain rate is non-negative. For the third variant, on compression the stress achieves the yield point, therefore the strain rate is less than or equal to zero. Thus, the system (2.16)–(2.18) can be solved numerically with the help of an search algorithm among a finite number of admissible variants. At each step of this algorithm, a linear system involving Eqs. (2.16) and equations corresponding to the variational inequalities (2.17), (2.18) is solved. Going to the next step is performed only if an obtained solution does not satisfy some restriction (inequality). In this case the corresponding equation is replaced with the alternative one. If all restrictions are satisfied, then the process of search is finished with going to the next time level.

To accelerate calculation, the multiple solution of the system (2.16) may be eliminated. To this end, all components of the vector $\boldsymbol{U}$ except stresses of plastic hinges are determined from Eqs. (2.16) and the equations for V_i^{k+1} involved in (2.17). Stresses of plastic hinges are assumed to be arbitrary. Strains of rigid contacts remain undetermined as well. More exactly, a basis of the space of solutions of the system of linear algebraic Eqs. (2.16), (2.17) is constructed. The dimension of this space must be equal to the number of rigid contacts and plastic hinges. This requirement is among the conditions of correctness of a rheological scheme. In practice this condition is easily verified. If the rank of a matrix consisting of the coefficients of the system is less than N_3 then the scheme is inappropriate.

Then the problem is reduced to the solution of the variational inequalities (2.17), (2.18) for stresses in plastic hinges and strains of rigid contacts with the help of the search algorithm described above. At each step of the algorithm the equations sets of dimension $N - N_2$ are solved. The requirement of existence and uniqueness of a solution of the variational inequalities as well as the condition of convergence of the algorithm impose additional restrictions on correctness of a scheme.

In the general case the system of linear algebraic equations, which follows from (2.16), (2.17), at the $(k + 1)$st time step has the form

$$\sum_{j=1}^{N_3} a_{ij}\, U_j^{k+1} = f_i^{k+1} - \sum_{j=N_3+1}^{N} a_{ij}\, U_j^{k+1}, \quad i = 1, \ldots, N_1,$$

$$\sum_{j=1}^{N_3} \bar{a}_{ij}\, U_j^{k+1} = \sum_{j=1} a_{ij}\, U_j^{k} - \sum_{j=N_3+1}^{N} a_{ij}\, U_j^{k+1}, \quad i = N_1+1, \ldots, N_2,$$

$$\sum_{j=1}^{N_3} a_{ij}\, U_j^{k+1} = V_i^{k+1} - \sum_{j=N_3+1}^{N} a_{ij}\, U_j^{k+1}, \quad i = N_2+1, \ldots, N_3,$$

where $\bar{a}_{ij} = a_{ij} - \Delta t\, \delta_{ij}$ (δ_{ij} is the Kronecker symbol). We assume that the determinant of the square matrix, composed of the coefficients in the left-hand side of this system, differs from zero. Thus, from the system we can express

$$U_i^{k+1} = \sum_{j=N_2+1}^{N} b_{ij}\, V_j^{k+1} + g_i^{k+1}, \quad i = 1, \ldots, N_3. \tag{2.19}$$

Here b_{ij} are the coefficients calculated from the coefficients a_{ij} and the inverse matrix of the system, g_j^{k+1} are the quantities depending on f_j^{k+1} and U_j^k, $V_j^{k+1} = U_j^{k+1}$ for $j = N_3+1, \ldots, N$.

Substituting Eqs. (2.19) into the inequalities (2.17), (2.18), we obtain a variational inequality in the matrix form with simple constraints (individual for each component of the unknown vector)

$$(\tilde{\mathbf{V}} - \mathbf{V})(\mathsf{C}\,\mathbf{V} - \mathbf{Y}) \geq 0, \quad \mathbf{V}^- \leq \mathbf{V} \leq \mathbf{V}^+, \quad \mathbf{V}^- \leq \tilde{\mathbf{V}} \leq \mathbf{V}^+, \tag{2.20}$$

where C and $\boldsymbol{Y}$ are a square matrix and a vector, respectively, (rows and columns are numbered beginning with N_2+1 rather than with 1) composed of the coefficients $c_{ij} = -b_{ij},\; y_i^{k+1} = g_i^{k+1}$ for $i = N_2+1, \ldots, N_3$ and

$$c_{ij} = \begin{cases} -\sum\limits_{l=1}^{N_3} a_{il}\, b_{lj}, & \text{if } j = N_2+1, \ldots, N_3, \\ -a_{ij} - \sum\limits_{l=1}^{N_3} a_{il}\, b_{lj}, & \text{if } j = N_3+1, \ldots, N, \end{cases}$$

$$y_i^{k+1} = \sum_{j=1}^{N_3} a_{ij}\, g_j^{k+1} - \sum_{j=1}^{N} a_{ij}\, U_j^k$$

for $i = N_3 + 1, \dots, N$. The components of the vector $\boldsymbol{V}^+$ corresponding to rigid contacts are equal to $+\infty$, for plastic elements $V_i^+ = U_i^*$. The vector $\boldsymbol{V}^-$ is composed of zeroes and negative quantities $-U_i^*$, respectively.

If the matrix C is positive definite then by the existence and uniqueness theorem (its proof is given in Sect. 3.2 of the next chapter) the variational inequality (2.20) has a unique solution. Numerical experiments with different rheological schemes show that the search process also converges. At the same time, for a wide class of schemes, in particular, for the scheme involving four rheological elements of different types considered above, the matrix C is nonnegative definite rather than positive definite. In this case the algorithm sometimes leads to infinitely repeating cycles. This situation can be improved by adding a small regularizing parameter to the diagonal elements which corresponds to involving a system of elastic elements of small rigidity in a rheological scheme in parallel with plastic hinges and rigid contacts. There is no assurance that a sequence of successive solutions converges as a regularization parameter tends to zero, however, it is sufficient to make an a posteriori convergence test by monotone decreasing the value of this parameter in computations.

This algorithm is implemented in the general form in the Delphy 5 object programming environment. The values of phenomenological parameters for elastic, viscous, and plastic elements are input variables for the computer system worked out. A scheme to be studied is constructed by tools of visual design with the use of graphic primitives. An example of the assignment of a concrete scheme involving four elements of different types is shown in Fig. 2.15. At the output the system enables one to obtain graphs of the strains and stresses variation in elements of a scheme depending on time as well as graphs of total strain $\varepsilon(t)$ and resulting stress $\sigma(t)$. Testing the algorithm was performed on the solutions obtained by the formulae (2.10), (2.11) and showed that the computational error of the algorithm corresponds to the first order of approximation of the implicit scheme.

The work technique with the system is as follows. To develop a new rheological scheme, one should choose an option or to press a key on the toolbar. In so doing, the scheme editor, i.e. a program dealing with a set of tools and objects with the help of which an arbitrary scheme is created, is started. Rheological elements are successively marked on a workspace with simultaneously specifying the parameters. A workspace is a space with a grid marked on it intended for the exact positioning of elements. For convenience, the so-called object inspector being a set of elements which can be placed in the workspace is located at the top right (Fig. 2.16). The object inspector has several editing fields which serve for the change of parameters and elements of a scheme. Thus, parameters of elements remain available for editing after they are introduced into a rheological scheme. It is sufficient to click the required elements and to change the corresponding values in the object inspector.

When placed in the workspace, an element can be stretched or compressed according to topology of a scheme. An element introduced mistakenly can be deleted or moved to other part of the workspace by the choice of corresponding option of the contextual menu which is defined for each element. The operation with elements can be also performed by "hot keys".

Fig. 2.16 Object inspector

The results of the assignment of a rheological scheme are saved in a file of special format formed by the system. Moreover, the system by itself keeps track of changes in a scheme and, if any, on exit a dialog window on its save is displayed. An alternative way of the assignment of a scheme, namely, loading from an existing file, is provided. When loading, a file name is displayed and file format is tested for compliance with the system.

Once the system has been defined, it should be pointed out which of two problems is to be solved (the problem on determining strain from given stress or, conversely, stress from given strain). The possibility to use time-dependent functions is realized with the help of a syntax analyzer of formulae. A syntax analyzer is a special function subprogram exported from a dynamic library involved in the project. A line with a formula and a list of values of the variables involved in the formula are transferred to the subprogram as parameters and at the output the calculated value of the function is obtained. The formula may involve the signs of mathematical operations (addition, subtraction, multiplication, division, raising to a power, extraction of a root) as well as all elementary functions.

Further computational procedures implementing this algorithm are started. In these procedures, a basis of the space of the solutions of the system (2.16) is constructed with the Gauss method with the choice of principal element. This method is also applied in the solution of the systems of equations which arise when implementing the variational inequality (2.20). Once computations have been performed, the system provides a possibility to output data in the form of graphs on a display or to an output file (a text file with separators) which can be used for analysis in other graphic editors.

The results of calculations obtained with the help of the computer system for the scheme involving four rheological elements (Fig. 2.14) are shown in Figs. 2.17–2.23. They represented in the form of diagrams of variation of strain with time for the cyclic loading with a constant and linearly increasing stress amplitude. On all graphs the curves 1 correspond to the time-dependence of stress $\sigma(t)$, the curves 2 to total strain $\varepsilon(t)$, and the curves 3 to strain $\varepsilon^c(t)$ of a rigid contact. The solution is given in the

Fig. 2.17 Loading for $\sigma(t) = -0.01 \cos t$

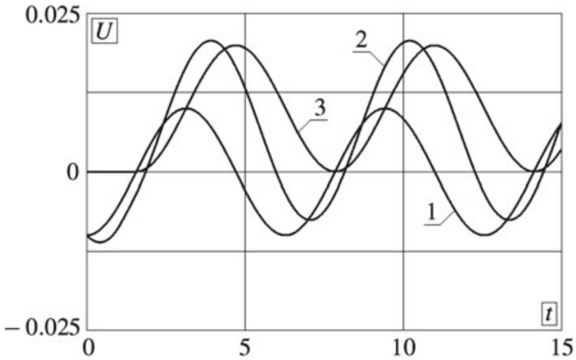

Fig. 2.18 Loading for $\sigma(t) = -0.001\,t \cos t$

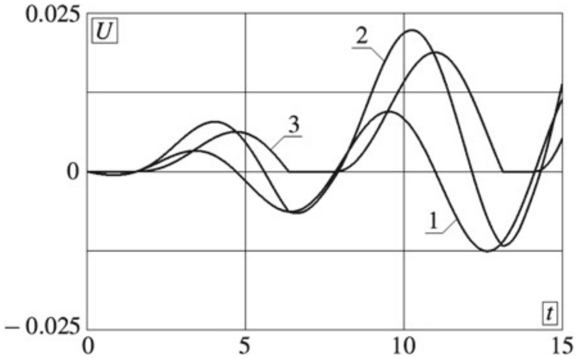

Fig. 2.19 Loading for $\sigma(t) = -0.001\,t \cos 2\,t$

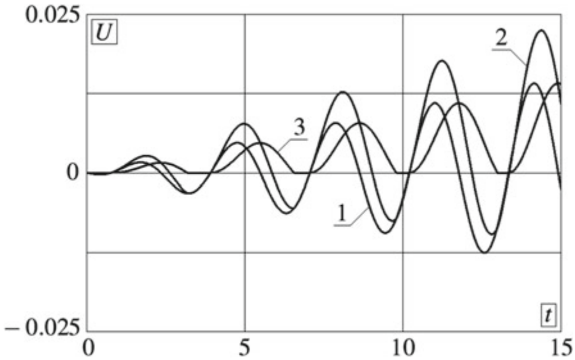

dimensionless variables ($\tau = a\,\eta$ is the characteristic time of relaxation):

$$\bar{t} = \frac{t}{\tau}, \quad \bar{\sigma} = a\,\sigma, \quad \bar{\varepsilon} = \varepsilon, \quad \bar{a} = 1, \quad \bar{\sigma}_s = a\,\sigma_s, \quad \bar{\eta} = \frac{a\,\eta}{\tau} = 1.$$

Fig. 2.20 Loading for $\sigma(t) = -0.001\, t \cos 3t$

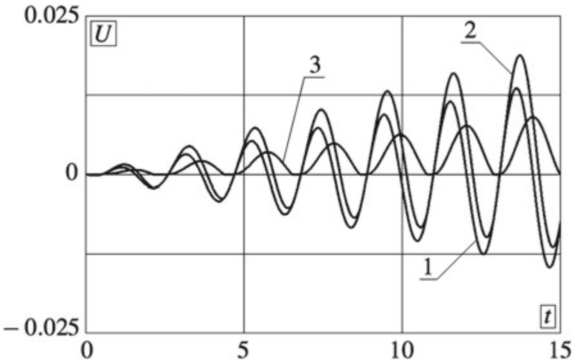

Fig. 2.21 Loading for $\sigma(t) = -0.001\, t \cos 5t$

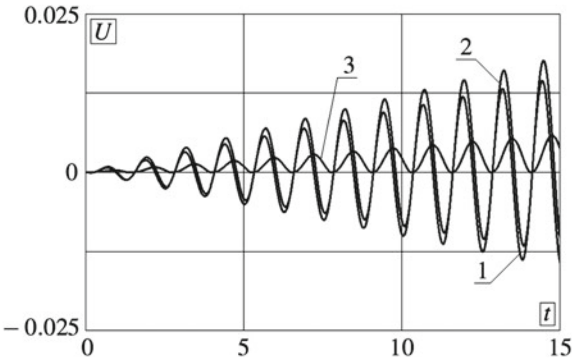

The dimensionless yield point $\bar{\sigma}_s$ (further a bar over dimensionless quantities is omitted) is equal to 0.005.

Analysis shows that for a constant amplitude a rigid contact is in a closed state only during the initial time interval within the first period of loading. Later on a medium adapts itself to the periodic load and never achieves a compaction mode (Fig. 2.17). In the case of an increasing amplitude, the interval of a closed state of a contact is periodically repeated (Figs. 2.18 and 2.19).

With increasing frequency (see Figs. 2.20 and 2.21), the curve 2 approaches to the curve 1. These curves can coincide exactly only in the case of a rheological scheme involving a single elastic element, hence, the influence of viscosity, plasticity, and heterostrength in comparison with elastic properties of a material becomes insignificant with increasing a loading frequency.

The graphs which describe variations of stresses and strains for the same rheological scheme with the same parameters for given total strain $\varepsilon(t)$ varying by a periodic law are given in Figs. 2.22 and 2.23. As before, the curves 1 correspond to time-dependence of stress and the curves 2—of strain. From the graphs of strain of a rigid contact (curves 3) it follows that a medium does not adapt itself to periodic de-

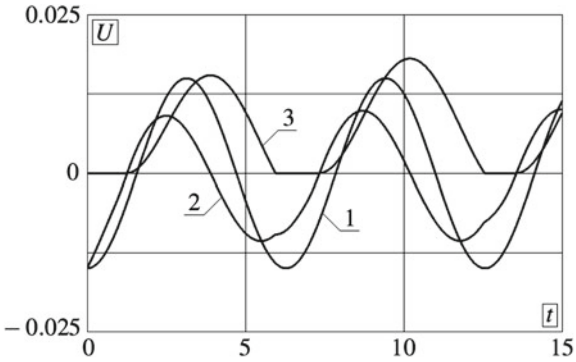

Fig. 2.22 Deformation for $\varepsilon(t) = -0.015 \cos t$

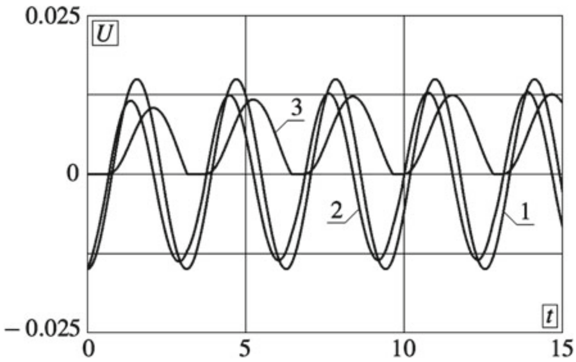

Fig. 2.23 Deformation for $\varepsilon(t) = -0.015 \cos 2t$

formation with a constant amplitude. At each cycle a compaction state of a medium where a contact is closed up is changed by a loosening state.

A comparison of Figs. 2.22 and 2.23 shows that with increasing a frequency the stress and strain curves approach to each other. Thus, in the case of a high-frequency deformation viscoplastic properties have a weak effect on a stress state of a material. An elastic element of a rheological scheme for which dimensionless dependencies $\sigma(t)$ and $\varepsilon(t)$ coincide is of first importance.

Other examples of the studies of rheological schemes for materials with different tensile and compressive strengths with the help of the computer system presented above are given in the following sections.

2.5 Fiber Composite Model

At the present level of development of a production technology of artificial materials, including those of engineering plastics, high-polymeric materials, and composites of various structures, rheology being a classical field of mechanics goes from the

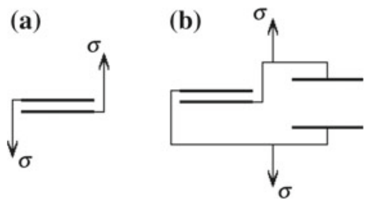

Fig. 2.24 Rheological scheme of a thread: **a** rigid contact of opposite polarity, **b** rigid contact with initial strain

solution of the direct problem of description of mechanical properties of existing materials to the study of the inverse problem of production of materials with preassigned properties. This approach requires development of new theoretical methods and improvement of known ones as well as software for mathematical modeling of the behaviour of continuous media which, at first glance, possess exotic properties. It seems likely that materials which are compression compliant more than tension compliant belong to this class.

A flexible non-stretchable thread (membrane) is the simplest example of a heteroresistant mechanical system without the compression strength and the tensile stress deformation. The stretched state is a natural state of a thread for zero strain and stress. Positive strain is impermissible, i.e. $\varepsilon \leq 0$, and negative stress is also impermissible, so $\sigma \geq 0$. If $\varepsilon < 0$ then $\sigma = 0$, and if $\sigma > 0$ then $\varepsilon = 0$. Thus, the constitutive relationships for a thread for uniaxial tension–compression coincide with the relationships (2.1) for an ideal granular medium accurate within the change of signs of the inequalities. The corresponding rheological scheme (Fig. 2.24a) is a rigid contact of opposite polarity.

When modeling finite strains of a thread, it is necessary to take into account restrictions from below related to the fact that, when changing positions of the ends in the compression process, a thread is stretched again. So, a more detailed rheological scheme must involve a rigid contact with a given value of initial strain (Fig. 2.24b). But this purpose is not pursued here.

A rheological scheme which describes the compression–tension process for a unidirectional fiber composite consisting of elastic-plastic fibres in a viscous binder is shown in Fig. 2.25. According to this scheme, with compression a sequential chain consisting of elastic and plastic elements is broken and only a viscous damper is deformed. By the Newton law in this case $\sigma = \eta\,\dot{\varepsilon}$. With tension, matched deformation of all elements takes place except for a rigid contact being in the closed state. For $\sigma \leq \sigma_s$ a plastic hinge also is not deformed, hence,

$$\sigma = \sigma^e + \sigma^v = \frac{\varepsilon}{a} + \eta\,\dot{\varepsilon}.$$

For $\sigma > \sigma_s$ stress in a chain equals σ_s, therefore

$$\sigma = \sigma_s + \sigma^v = \sigma_s + \eta\,\dot{\varepsilon}, \quad \varepsilon^e = a\,\sigma_s, \quad \varepsilon^p = \varepsilon - \varepsilon^e.$$

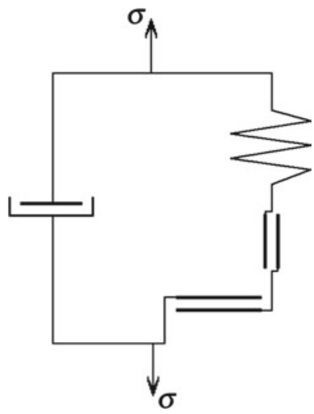

Fig. 2.25 Rheological scheme of a composite

Stresses and strains of all elements are uniquely determined in any version of loading considered here. Thus, this system is correct.

Results of computations for this scheme are given in Figs. 2.26–2.29, [25]. A series of creep diagrams for a constant stress level $\sigma = \pm 0.015, \pm 0.01$, and ± 0.005 (the curves $1, \ldots, 6$, respectively) is presented in Fig. 2.26. For compressive stresses the diagrams are linear, they describe the strain of a viscous element. For tensile stresses the curves are of nonlinear nature, besides, on the initial segment where their convexity is more pronounced elastic deformation takes place and with arising plastic deformation the curves become more flat. The stress relaxation diagrams for strain $\varepsilon(t) = \varepsilon_0\left(1 - e^{-3t}\right)$ which exponentially tends to a constant value ε_0 are shown in Fig. 2.27. Here the curves $1, \ldots, 6$ correspond to $\varepsilon_0 = \pm 0.015, \pm 0.01$, and ± 0.005, respectively. The salient points on the upper graphs correspond to going from an elastic stage of the fibres tension to a plastic one. Observe that with compression stresses are rapidly reduced to zero whereas with tension they relax to a constant value equal to the yield point of a plastic hinge. It turns out that for a moderate level of tensile strain ε_0, when a hinge remains in the rigid state, dimensionless stress $\sigma_0 = \varepsilon_0$ of an elastic spring is the limit value in the relaxation process.

Results of calculation for the uniaxial cyclic loading and the cyclic deformation of a composite are shown in Figs. 2.28 and 2.29. The curves 1 correspond to the dependence $\sigma(t)$, the curves 2 characterize the dependence $\varepsilon(t)$, the curves 3 describe the variation of strain of a rigid contact with time, and the curves 4 describe the variation of strain of a plastic element. Analysis shows that plastic strain takes place only in the first cycle of loading or deformation of a material. After irreversible elongation the fibres remain elastic in all subsequent cycles.

Consider a more complicated rheological scheme of a fiber composite which is heteroresistant with respect to tension and compression (Fig. 2.30). A coupled chain of elastic and plastic elements in this scheme serves to model a double system of reinforcing fibres differing in elastic and plastic properties which show themselves only with tension. As in the previous scheme, compression of a composite is de-

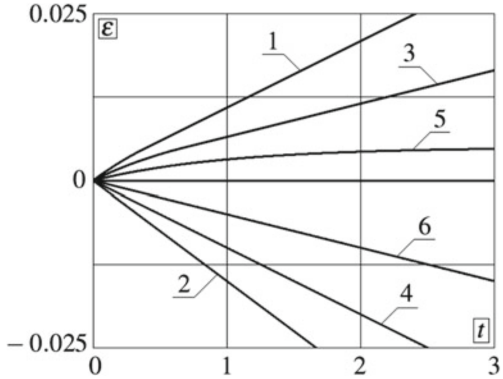

Fig. 2.26 Creep diagrams

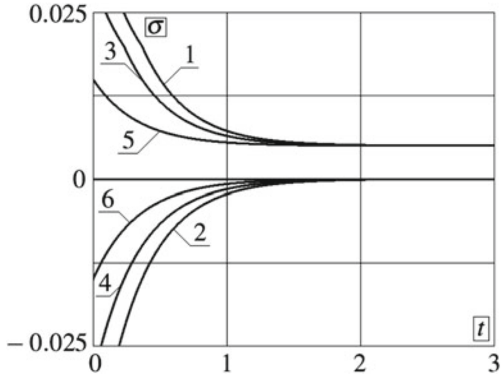

Fig. 2.27 Stress relaxation curves

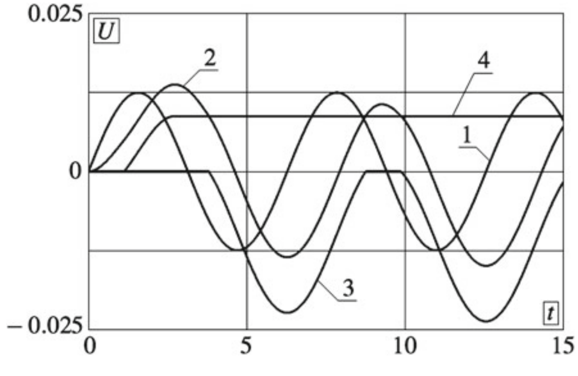

Fig. 2.28 Loading for $\sigma(t) = 0.0125 \sin t$

scribed by a model of a viscous medium. With tension, one of three alternatives is implemented. If strain does not exceed the critical value equal to min $\{a\,\sigma_s, a'\sigma_s'\}$ where a, a' and σ_s, σ_s' are the moduli of elastic compliance and the yield points of elements, respectively, then visco-elastic deformation of a material takes place according to the Kelvin–Voigt theory:

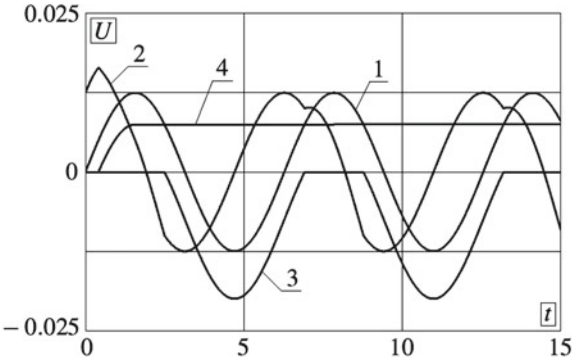

Fig. 2.29 Deformation for $\varepsilon(t) = 0.0125\,\sin t$

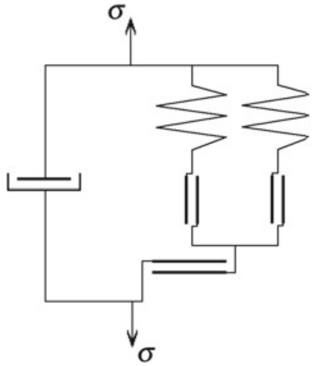

Fig. 2.30 A double system of fibres

$$\sigma = \left(\frac{1}{a} + \frac{1}{a'}\right)\varepsilon + \eta\,\dot{\varepsilon}.$$

Exceeding a critical level results in the fact that in the chain with a lesser value of the product $a\,\sigma_s$ a plastic hinge is broken. In this case

$$\sigma = \sigma_s + \frac{\varepsilon}{a'} + \eta\,\dot{\varepsilon}, \quad a\,\sigma_s < \varepsilon \le a'\sigma_s'.$$

Finally, if strain is higher than $a'\sigma_s'$ then both hinges are broken. In this case the constitutive equation has the form:

$$\sigma = \sigma_s + \sigma_s' + \eta\,\dot{\varepsilon}.$$

Thus, the active loading takes place for $\dot{\varepsilon} \ge 0$. When unloading, for $\dot{\varepsilon} < 0$, both hinges are simultaneously blocked. The increments of total stress and strain satisfy the equation

$$\mathrm{d}\sigma = \left(\frac{1}{a} + \frac{1}{a'}\right)\mathrm{d}\varepsilon + \eta\,\mathrm{d}\dot{\varepsilon},$$

Fig. 2.31 Creep diagrams

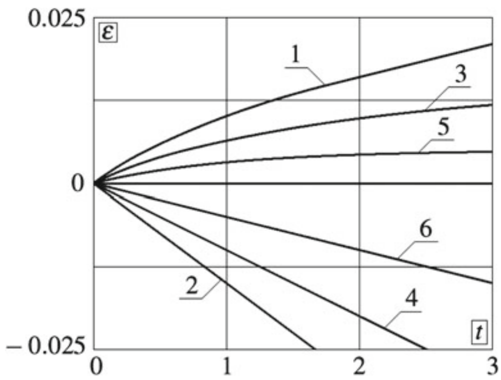

Fig. 2.32 Stress relaxation curves

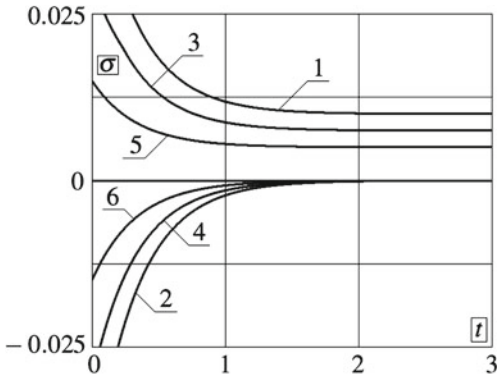

from which it follows that

$$\sigma = \sigma_s + \sigma_s' + \left(\frac{1}{a} + \frac{1}{a'}\right)(\varepsilon - \varepsilon_{\max}) + \eta\,\dot{\varepsilon},$$

where $\varepsilon_{\max}$ is the maximal tensile strain achieved at the loading stage. A rigid contact is broken if stress $\sigma^c = \sigma - \eta\,\dot{\varepsilon}$ calculated by this formula becomes zero in the unloading process. Further deformation for $\dot{\varepsilon} < 0$ is described by the Newton equation.

One can make sure that in each of these variants stresses and strains of all elements of the rheological scheme are uniquely determined, so this scheme is correct. In Figs. 2.31 and 2.32, the diagrams of creep and stress relaxation similar to those in Figs. 2.26 and 2.27 are presented. The results are obtained with the help of the computer system for the following values of the dimensionless parameters of the model: $a = a' = 2$, $\sigma_s = 0.0025$, $\sigma_s' = 0.0075$. Comparison of the diagrams shows that under tension of a material with a double reinforcing system the rigidity essentially increases. Besides, the level of residual stresses after relaxation increases.

Including additional elements in the rheological schemes considered above enables one to take into account elastic and plastic properties of a composite binder as well as viscous properties of reinforcing fibers.

2.6 Porous Materials

A number of books (see bibliography of [3–5, 10, 15, 20]) is devoted to the mathematical modeling of behavior of porous materials under the action of static and dynamic loads. However, up to now there has been no unique theory. Main difficulties here are related to the fact that porous materials also have the heteroresistance property. Under the action of compressive stresses up to the instant of collapse of pores these materials turn out to be more compliant than with subsequent compression. The unloading process for a compressed porous medium may be reversible or irreversible. In the first case a pore space restores completely for zero stress and in the second case in the limits of the "loading–unloading" cycle pores vary in size, [19, 29]. Collapse of pores can be modeled as a result of loss of stability of a porous sceleton, [6, 11].

New application of mechanics of porous materials is porous metals. These artificial materials can be widely used in engineering because of their low density and good damping properties, [16]. The ability of porous metals effectively absorb mechanical energy on the stage of plastic deformation opens up prospects for their use in the manufacture of bumper cars and elements of the car body, the so-called crushed zones. They also can be used in gearboxes and actuators as destructible fuses which dissipate the energy of dynamic impact preventing the destruction of all mechanical system.

Deformation properties of porous metals are significantly different in tension and in compression. In tension there are the stage of elastic deformation of skeleton and the stage of plastic flow up to the destruction. In compression there are the stages of elastic and plastic deformation of skeleton until the collapse of pores and the subsequent stage of elastic or elastic-plastic deformation of a solid material without pores. At small sizes of pores the collapse can occur on the elastic stage with the appearance of plasticity only under a sufficiently high level of load.

At present the technologies of production of metal foams based on aluminum, copper, nickel, tin, zinc and other metals are developed. According to the information published in Internet, A. Rabiney from the University of North Carolina (USA) in 2010 created a technology for production of the most durable foam in the world. High strength of this material is achieved by ensuring that the surface of a thin-wall skeleton in the foam practically has no dislocations, i.e. defects that are initiators of the destruction.

Extensive experimental researches of the mechanical properties of such a materials were carried out. The diagrams of uniaxial tension and uniaxial compression on the example of aluminum foam and porous copper were obtained, [1, 2]. The problems of durability and cyclic fatigue of porous metals are considered in [17] etc.

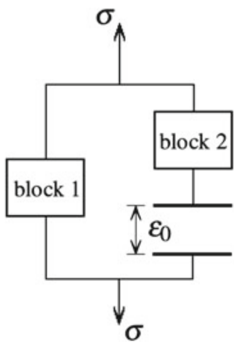

Fig. 2.33 General scheme of porous material

Theoretical questions of the constructing constitutive equations and of the analysis on this basis the spatial stress-strain state of structural elements of metal foams, according to the available publications, have not been studied almost. At the level of physical and mechanical representations, the deformation of metal foam is rather complex process. Under compression it leads to the elastic-plastic loss of stability of metal skeleton at high porosity and to the stable mechanism of collapse of pores at low porosity. The collapse is accompanied by a contact interaction of skeleton walls which is difficult for modeling at the discrete level. Besides, it is necessary to consider the presence of compressed gas in closed pores. It is rather difficult to describe the process of shear when, according to the experiments, the volume of a material changes. Even more difficult to construct a universal model of the spatial stress-strain state of a material under complex loading. The performance of adequate computations based on discrete models of the metal foam as a structurally inhomogeneous material is only possible with the use of multiprocessor systems with high performance and large amount of random-access memory.

A simple and effective solution to these problems gives the rheological approach, in the framework of which one can describe the main qualitative and quantitative effects such as a significant difference of diagrams of uniaxial deformation before and after the collapse of pores and a significant dissipation of energy at the stage of plastic flow of a material.

A rheological scheme of the general form for a porous material is shown in Fig. 2.33. Here block 1 consisting of elements placed parallel to a prestretched rigid contact describes mechanical properties of a skeleton with open pores. Initial strain ε_0 of a rigid contact is defined by a specific volume of pores. Block 2 which consists of elements placed in series with a rigid contact describes the hardening of a compressed skeleton. In a more general case, one more block of rheological elements modeling strain of a medium which does not depend on a pores state can be added to this scheme in series, [24].

Replacing blocks 1 and 2 with elastic springs, we obtain the simplest model of the ideal elastic porous medium whose rheological scheme is given in Fig. 2.34a. According to this model, with tension of a material and with compression to the critical value $\varepsilon = -\varepsilon_0$ of strain the equation $\sigma = \varepsilon/a$ holds, with compression

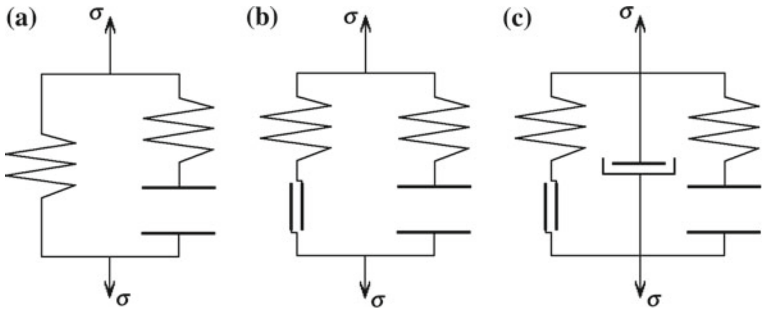

Fig. 2.34 Rheological schemes of porous materials: **a** elastic material, **b** elastic-plastic material, **c** elastic-visco-plastic material

Fig. 2.35 Diagrams of uniaxial tension–compression: **a** elastic porous material, **b** elastic-plastic porous material in the case of elastic collapse of pores

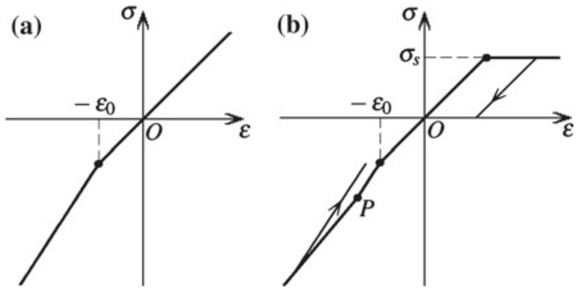

over the critical value ($\varepsilon < -\varepsilon_0$) the equation $\mathrm{d}\sigma = (1/a + 1/b)\,\mathrm{d}\varepsilon$ holds (a and b are moduli of elastic compliance of springs). The deformation process for such a medium is thermodynamically reversible. A diagram of uniaxial tension–compression is shown in Fig. 2.35a as a two-segment broken line.

A rheological scheme of an elastic-plastic porous material, where the compression process after collapse of pores is described with the model of linear hardening, is presented in Fig. 2.34b. If stress in modulus does not exceed the yield point σ_s of a plastic hinge, then deformation of a material exactly corresponds to the elastic model. It is impossible to apply tensile stress higher than σ_s since for $\sigma = \sigma_s$ flow of a material due to increase of size of pores is observed. With compression the effect of plastic hardening takes place.

Typical diagrams of the active loading and unloading are shown in Figs. 2.35b and 2.36a. Figure 2.35b corresponds to the case where the phenomenological parameters satisfy the condition $\varepsilon_0 < a\,\sigma_s$. This condition holds for weakly porous materials with small value of ε_0 and means that the process of collapse of pores takes place in the range of elastic strain. According to this scheme, at the point P of the transition of a medium to the plastic state

$$\sigma = \frac{\varepsilon}{a} + \frac{\varepsilon + \varepsilon_0}{b}, \quad \frac{\varepsilon}{a} = -\sigma_s.$$

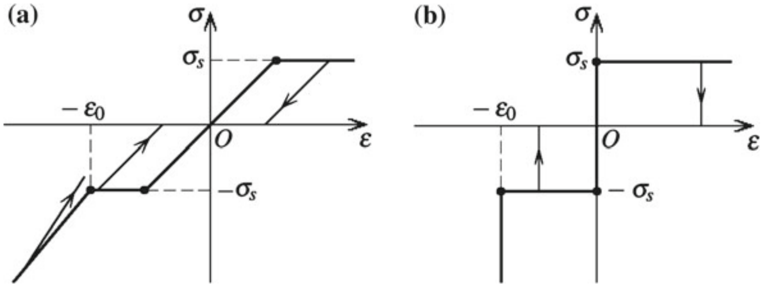

Fig. 2.36 Diagrams of uniaxial tension–compression in the case of plastic collapse of pores: **a** elastic-plastic material, **b** rigid-plastic material

Hence, at this point $\sigma = -\sigma_s(1 + a/b) + \varepsilon_0/b$. The effect of the plastic hardening of a compressed skeleton is described by the linear equation

$$\sigma = -\sigma_s + \frac{\varepsilon + \varepsilon_0}{b}.$$

The case of $\varepsilon_0 > a\,\sigma_s$, where compression of pores is accompanied by plastic dissipation of energy, is considered in Fig. 2.36a. It should be noted that the tangent of the angle of slope of the segment, which corresponds to the unloading of a plastically compressed material, equals $1/a$ until the instant of collapse of pores and after this instant it increases to $1/a + 1/b$.

Using the rheological scheme given in Fig. 2.34b, with a tending a to zero, we can obtain a model in which strain of pores is completely irreversible and strain of a compressed skeleton follows the law of linear hardening. With b tending to zero, a model of an elastic-plastic porous medium with an absolutely rigid skeleton is obtained. If $a \to 0$ and $b \to 0$ simultaneously, then a model of a rigid-plastic porous medium with a rigid skeleton, whose diagram of uniaxial deformation is given in Fig. 2.36b, can be obtained.

The diagrams show that the constitutive relationships of an elastic-plastic porous medium are as much incorrect in the mechanical sense as ones of the classical theory of ideal plasticity. To obtain an unambiguous description of deformation of a material for a given loading program, we add a regularizing viscous element to the scheme (see Fig. 2.34c). The model corresponding to this scheme takes into account viscous properties of the skeleton. With η tending to zero, it is transformed into a model of an elastic-plastic porous medium.

Graphs of the changing of resulting stress (the curve 1) and stress in a rigid contact (the curve 2) for cyclic deformation of a medium with zero viscosity are presented in Fig. 2.37. The results are obtained for $a = b = 1$, $\sigma_s = 0.005$, and $\varepsilon_0 = 0.0025$. This choice of the parameters corresponds to the case of elastic collapse of pores. However, according to computations elastic collapse takes place only at the first cycle. At the second and subsequent cycles, specific horizontal portions of compressive stresses corresponding to the value of the yield point of a plastic hinge

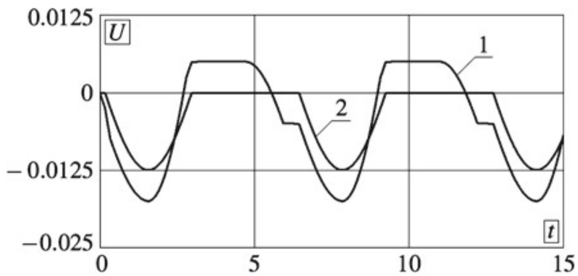

Fig. 2.37 Deformation for $\varepsilon(t) = -0.015 \sin t$ ($\varepsilon_0 = 0.0025$)

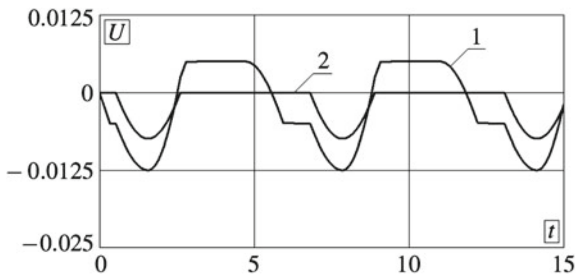

Fig. 2.38 Deformation for $\varepsilon(t) = -0.015 \sin t$ ($\varepsilon_0 = 0.0075$)

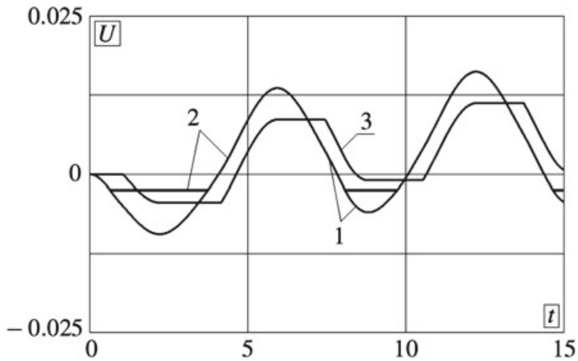

Fig. 2.39 Loading for $\sigma(t) = -0.015 \sin t$ ($\varepsilon_0 = 0.0025$)

appear on the curve 1 as a result of preliminary irreversible strain of a material. According to the curve 2, in this case a rigid contact is in the broken state since its stress turns out to be zero. Thus, even at the second cycle compression of pores is accompanied by plastic strain of a material.

Similar graphs for $\varepsilon_0 = 0.0075$ in the case of plastic collapse at the first cycle of the deformation program are shown in Fig. 2.38. Comparison shows that as the porosity increases, the level of compressive stresses in a medium considerably decreases.

Graphs of the changing of characteristics of the strained state for a viscoplastic porous medium with the dimensionless viscosity coefficient $\eta = 1$ for the cyclic loading are shown in Figs. 2.39 and 2.40. The curves 1 describe total strain $\varepsilon(t)$, the curves 2 describe strain of a rigid contact, and the curves 3 describe strain of a plastic

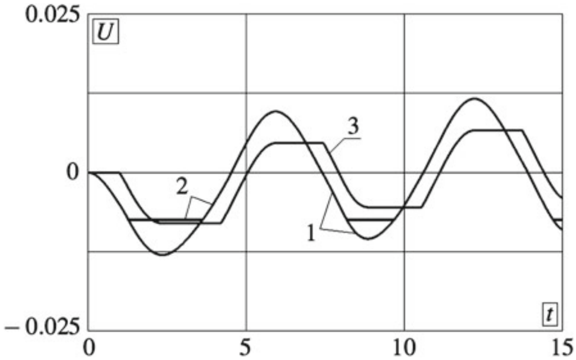

Fig. 2.40 Loading for $\sigma(t) = -0.015 \sin t$ ($\varepsilon_0 = 0.0075$)

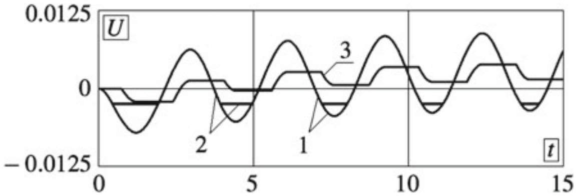

Fig. 2.41 Loading for $\sigma(t) = -0.015 \sin 2t$ ($\varepsilon_0 = 0.0025$)

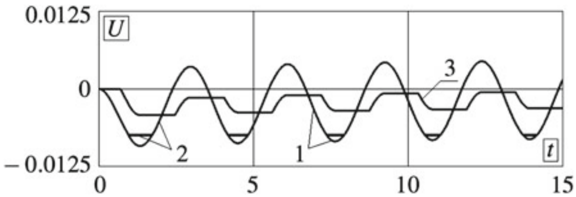

Fig. 2.42 Loading for $\sigma(t) = -0.015 \sin 2t$ ($\varepsilon_0 = 0.0075$)

element. Fig. 2.39 corresponds to the case of $\varepsilon_0 < a\,\sigma_s$ and Fig. 2.40 corresponds to the case of $\varepsilon_0 > a\,\sigma_s$. In the first case plastic strain of a medium is observed after the instant of collapse of pores and in the second case until this instant. However, as before, this holds true only for the first cycle of loading, at all subsequent cycles the compression of open pores is accompanied by plastic dissipation of energy. From the presented graphs it follows that strain of a rigid contact differs from total strain only when a contact is closed. In addition, the interval of the closed state decreases depending on the number of a cycle and for a sufficiently large value of time corresponding graphs completely coincide. Hence, for the multiple cyclic loading a material gradually loses the heteroresistance property and collapse of pores comes to a stop. Analysing the curves, we can notice that in a viscous medium the creep is developed with time, i.e. the maximal value of strain increases during one cycle.

Similar graphs for the cyclic loading with doubled frequency (in comparison with the graphs shown in Figs. 2.39 and 2.40) are represented in Figs. 2.41 and 2.42.

To conclude, we notice that a large series of methodical calculations performed with the help of the computer system described above shows that as frequency of the cyclic loading increases, the level of strain of a medium considerably decreases, a given stress amplitude turns out to be insufficient to provide collapse of pores, plastic strain takes a negative value and remains constant during all loading process, and the creep property completely disappears. In this case the behaviour of a porous material is adequately described by the elasticity theory with initial (plastic) strain taken into account.

2.7 Rheologically Complex Materials

In the previous sections, constitutive relationships of uniaxial deformation of materials with different strengths were constructed only on the basis of the method of rheological schemes where four types of elements associated with elementary properties are used. If in a tension or compression state a material shows complicated set of properties, then one has to use a large number of rheological elements to describe it. This results in a multiparametric model which may be difficult of access for practical applications. An alternative approach which is well-developed in the application to standard viscoelastic materials with symmetric properties with respect to tension and compression, [12, 14, 21], is as follows. Constitutive equations are postulated in the special form for which, generally speaking, there exists no appropriate rheological scheme. Generalizing this approach to materials with different strengths we notice that, in combination with a system of rigid contacts, in a nonstandard rheological scheme blocks, which have no traditional rheological schemes, may be used along with blocks involving traditional elements. For example, in a general scheme of a porous material shown in Fig. 2.33, constitutive equations of the special form mentioned above may correspond to the blocks 1 and 2. Similar conditional schemes can be constructed for the description of composite and granular materials. However, this way of the construction of constitutive relationships has some restrictions. One of the most important restrictions is related to the requirement of dissipativity of the derivable model.

For a model with the standard rheological scheme involving an arbitrary number of elements of four types the dissipativity property holds automatically. In the classical viscoelasticity theory this statement is assumed to be obvious since by the physical sense dissipation of energy in a system is formed from dissipations on its elements. We prove it more rigorously basing on the formal representation of rheological schemes given in Sect. 2.4.

In the general case the sum of stress powers of elements of a rheological scheme for corresponding strains is expressed by the next formula:

$$\dot{W} = \sum_{j=1}^{n} \sigma_j \, \dot{\varepsilon}^{\,j}, \quad \varepsilon^j = \sum_{k=b_j}^{e_j} \varepsilon_k.$$

Here, when calculating strain of the j-th element, the summation is performed over the layers of a scheme numbered from b_j where the element begins to e_j where it ends. Collecting similar terms, we can rewrite the expression for $\dot{W}$ in the form of a linear combination of strain rates of layers

$$\dot{W} = \sum_{k=1}^{m} \bar{\sigma}_k \, \dot{\varepsilon}_k$$

with the coefficients $\bar{\sigma}_k$ equal to the sum of stresses of those elements whose ends pass through the given layer. In view of the equilibrium equation, at the upper boundary of the first layer $\bar{\sigma}_1 = \sigma(t)$. To show that the remaining coefficients are equal to $\sigma(t)$ as well, we break in mind the ends of elements intersecting the interfaces between layers and add paired systems of stresses σ_j and $-\sigma_j$, which are equivalent to zero, to the corresponding boundaries. From the equilibrium equations written for interfaces we successively obtain

$$\bar{\sigma}_1 = \bar{\sigma}_2, \quad \bar{\sigma}_2 = \bar{\sigma}_3, \quad \ldots, \quad \bar{\sigma}_{m-1} = \bar{\sigma}_m.$$

Finally, we have

$$\dot{W} = \sigma \sum_{k=1}^{m} \dot{\varepsilon}_k = \sigma \, \dot{\varepsilon}.$$

Among rheological elements of four types, two elements (an elastic spring and a rigid contact) represent conservative systems. For them

$$\sigma_j \, \dot{\varepsilon}^{\,j} = \dot{\Phi}_j\big(\varepsilon^j\big),$$

where Φ_j are the corresponding stress potentials. The remaining two elements (a viscous damper and a plastic hinge) are dissipative because for them

$$\sigma_j \, \dot{\varepsilon}^{\,j} = D_j\big(\dot{\varepsilon}^{\,j}\big) \geq 0.$$

Thus, the dissipativity property of a model consists in the following equality:

$$\sigma \, \dot{\varepsilon} = \dot{\Phi} + D, \tag{2.21}$$

where the functions Φ and $D \geq 0$ are the sums of conservative and dissipative potentials of the elements of a scheme.

Now consider the case of a nonstandard rheological scheme. Repeating the above considerations, we can show that a model of uniaxial tension–compression is dissipative if and only if all blocks involved in the scheme are dissipative. Keeping in mind applications to granular materials, for description of which it makes sense to use mathematical models of the hereditary elasticity theory as individual blocks in combination with standard rheological elements, we present an independent derivation of the dissipation condition for such block in the Breuer and Onat form, [7, 21].

Assume that the constitutive equation of a model is written in the convolution form

$$\sigma(t) = (\varphi * \varepsilon)(t) \equiv \int_{-\infty}^{t} \varphi(t - t_1)\, \varepsilon(t_1)\, \mathrm{d}t_1. \tag{2.22}$$

Here the relaxation kernel $\varphi(t)$ is an arbitrary function constructed from experimental data. We can extend this function putting it equal to zero for negative values of t, since (2.22) involves only the values corresponding to $t \geq 0$. Then Eq. (2.22) is reduced to the form

$$\sigma(t) = \int_{-\infty}^{\infty} \varphi(t - t_1)\, \varepsilon(t_1)\, dt_1 = \int_{-\infty}^{\infty} \varphi(t_2)\, \varepsilon(t - t_2)\, \mathrm{d}t_2 = (\varepsilon * \varphi)(t).$$

It is known that the Fourier transform

$$\widehat{\sigma}(\omega) = \int_{-\infty}^{\infty} \sigma(t)\, e^{-\imath\, \omega\, t} \mathrm{d}t$$

of the convolution of two functions, one of which vanishes for $t < 0$, is the product of the Fourier transform. Therefore the equality

$$\widehat{\sigma}(\omega) = \widehat{\varphi}(\omega)\, \widehat{\varepsilon}(\omega)$$

is valid. Hence, Eq. (2.22) can be represented in the inverted form

$$\varepsilon(t) = (\psi * \sigma)(t), \tag{2.23}$$

where $\psi(t)$ is the creep kernel being a function which is put to be equal to zero for negative t and for which $\widehat{\psi}(\omega) = 1\big/\widehat{\varphi}(\omega)$.

For the Kelvin–Voigt classical model $\widehat{\varphi}(\omega) = 1/a + \imath\, \omega\, \eta$. For the Maxwell model $\widehat{\varphi}(\omega) = 1\big/\big(a + 1/(\imath\, \omega\, \eta)\big)$. For the parallel connection of two blocks of elastic and viscous elements, the Fourier transform of the relaxation kernel is equal to the sum of the Fourier transforms of the kernels of the blocks. For the series connection it is equal to the reciprocal value of the sum of the reciprocal values. Hence, in the case of a viscoelastic scheme of the general form the quantity $\widehat{\varphi}(\omega)$ is a fractionally rational complex-valued function $P(\imath\, \omega)/Q(\imath\, \omega)$ for which the difference of degrees of the polynomials $P(z)$ and $Q(z)$ does not exceed one.

If in the constitutive Eq. (2.23) $\varepsilon(t)$ is a periodic function with period T then the function $\sigma(t)$ is also periodic with the same period. According to the second principle of thermodynamics, the energy produced by stress per one deformation period (cycle) can not be negative, i.e.

$$W = \int_0^T \sigma(t)\, d\varepsilon(t) \geq 0. \tag{2.24}$$

If this property is violated, then a mathematical model with the constitutive Eqs. (2.22), (2.23) is incorrect in the physical sense, since in its framework there exists "perpetuum mobile". Expand an arbitrary periodic function into the Fourier series

$$\varepsilon(t) = \frac{c_0}{2} + \sum_{k=1}^{\infty} \bigl(c_k\ \cos\omega_k t + s_k\ \sin\omega_k t\bigr),$$

where $\omega_k = 2\pi\, k/T$. For an individual term of the type $\varepsilon_k(t) = \sin\omega_k t$ the inequality (2.24) takes the following form:

$$W_k = \omega_k \int_0^T \sigma_k(t) \cos\omega_k t\ \mathrm{d}t = \omega_k\, \Re \int_0^T \sigma_k(t)\, e^{\imath\omega_k t}\ \mathrm{d}t \geq 0.$$

Here the fact that the value of stress is real is taken into account. Due to Eq. (2.22)

$$\begin{aligned}
\sigma_k(t) &= \int_{-\infty}^{\infty} \varphi(t - t_1) \sin\omega_k t_1\ \mathrm{d}t_1 = \int_{-\infty}^{\infty} \varphi(t - t_1) \frac{e^{\imath\omega_k t_1} - e^{-\imath\omega_k t_1}}{2\imath}\ \mathrm{d}t_1 \\
&= \frac{e^{\imath\omega_k t}}{2\imath} \int_{-\infty}^{\infty} \varphi(t - t_1)\, e^{-\imath\omega_k (t - t_1)}\ \mathrm{d}t_1 - \frac{e^{-\imath\omega_k t}}{2\imath} \int_{-\infty}^{\infty} \varphi(t - t_1)\, e^{\imath\omega_k (t - t_1)}\ \mathrm{d}t_1 \\
&= \frac{e^{\imath\omega_k t}}{2\imath}\, \widehat{\varphi}(\omega_k) - \frac{e^{-\imath\omega_k t}}{2\imath}\, \widehat{\varphi}(-\omega_k).
\end{aligned}$$

The complex-conjugate value is calculated by the formula

$$\overline{\sigma_k(t)} = -\frac{e^{-\imath\omega_k t}}{2\imath}\, \overline{\widehat{\varphi}(\omega_k)} + \frac{e^{\imath\omega_k t}}{2\imath}\, \overline{\widehat{\varphi}(-\omega_k)}.$$

Stress turns out be real, i.e. $\sigma_k(t) = \overline{\sigma_k(t)}$, provided that

$$\overline{\widehat{\varphi}(\omega)} = \widehat{\varphi}(-\omega). \tag{2.25}$$

In particular, from this condition it follows that if $\widehat{\varphi}(\omega)$ is a fractionally rational function then $P(z)$ and $Q(z)$ must be polynomials with real coefficients. The immediate calculation of the integral

$$\int_0^T \sigma_k(t)\, e^{\imath\omega_k t}\, dt = \frac{\imath\, T}{2}\, \widehat{\varphi}(-\omega_k)$$

enables one to determine

$$W_k = \frac{\omega_k\, T}{2}\, \Im\, \widehat{\varphi}(\omega_k) = \pi\, k\, \Im\, \widehat{\varphi}(\omega_k)$$

taking into account (2.25). For a term of the type $\varepsilon_k(t) = \cos\omega_k t$ stress is determined by the formula

$$\sigma_k(t) = \frac{e^{\imath\omega_k t}}{2}\, \widehat{\varphi}(\omega_k) + \frac{e^{-\imath\omega_k t}}{2}\, \widehat{\varphi}(-\omega_k).$$

It also is real provided that the condition (2.25) holds. The value of the energy dissipation per one deformation cycle is calculated as the integral

$$W_k = -\omega_k \int_0^T \sigma_k(t)\sin\omega_k t\, dt = \omega_k\, \Im \int_0^T \sigma_k(t)\, e^{-\imath\omega_k t}\, dt.$$

Considering that $\int_0^T \sigma_k(t)\, e^{-\imath\omega_k t}\, dt = \frac{\imath\, T}{2}\, \widehat{\varphi}(\omega_k)$, we arrive at the previous expression for W_k.

Thus, the condition of non-negativity of internal dissipation of energy for individual harmonics of the Fourier series is reduced to Eq. (2.25) and the inequality

$$\Im\, \widehat{\varphi}(\omega) \geq 0. \tag{2.26}$$

To write it for an arbitrary deformation program, we represent the Fourier series in the complex form

$$\varepsilon(t) = \sum_{k=-\infty}^{\infty} a_k\, e^{\imath\omega_k t}, \quad a_k = \frac{1}{T}\int_0^T \varepsilon(t) e^{-\imath\omega_k t}\mathrm{d}t.$$

Here $a_0 = c_0/2$ and $a_k = \big(c_k - \imath\, s_k\big)/2$, $a_{-k} = \big(c_k + \imath\, s_k\big)/2$ for $k = 1, 2, \ldots$. Because of (2.22), stress is expanded into the series

$$\sigma(t) = \sum_{l=-\infty}^{\infty} a_l \int_{-\infty}^{\infty} \varphi(t - t_1)\, e^{\omega_l t_1}\mathrm{d}t_1 = \sum_{l=-\infty}^{\infty} a_l\, \widehat{\varphi}(\omega_l)\, e^{\imath\omega_l t}.$$

Taking into account orthogonality of the system of the functions $e^{\imath\omega_l t}$ on the segment $[0, T]$, the inequality (2.24) can be written in the form:

$$0 \leq W = \imath \sum_{k,l=-\infty}^{\infty} a_k\, a_l\, \omega_k\, \widehat{\varphi}(\omega_l) \int_0^T e^{\imath(\omega_k+\omega_l)t} \mathrm{d}t = \imath\, T \sum_{k=-\infty}^{\infty} a_k\, a_{-k}\, \omega_k\, \widehat{\varphi}(-\omega_k)$$

$$= \frac{\imath\, T}{4} \sum_{k=1}^{\infty} \big(c_k^2 + s_k^2\big)\omega_k \big(\widehat{\varphi}(-\omega_k) - \widehat{\varphi}(\omega_k)\big).$$

It holds automatically provided that the conditions (2.25) and (2.26) are valid since

$$\imath\big(\widehat{\varphi}(-\omega_k) - \widehat{\varphi}(\omega_k)\big) = \imath\, \big(\overline{\widehat{\varphi}(\omega_k)} - \widehat{\varphi}(\omega_k)\big) = 2\, \Im\, \widehat{\varphi}(\omega_k)$$

and, hence, $W = \sum_{k=1}^{\infty} \big(c_k^2 + s_k^2\big) W_k$.

Considering that the period T is arbitrary, we can make the following conclusion: a model of a linear hereditary medium with a relaxation kernel $\varphi(t)$ is dissipative if and only if the Eq. (2.25) and the inequality (2.26) are valid for any $\omega > 0$. In terms of a creep kernel this system of conditions is written as

$$\overline{\widehat{\psi}(\omega)} = \widehat{\psi}(-\omega), \quad \Im\, \widehat{\psi}(\omega) \leq 0.$$

In an equivalent form the inequality (2.26) was first obtained by Breuer and Onat from other considerations related to the fact that work of stresses on strains, which are identically equal to zero for $t \leq 0$, is positive. For viscoelastic materials whose constitutive equations are constructed with the help of standard rheological schemes this inequality holds automatically since integration of Eq. (2.21) within the limits of one cycle yields

$$\int_0^T \sigma(t)\, \mathrm{d}\varepsilon(t) = \int_0^T D(t)\, \mathrm{d}t \geq 0.$$

The inequality of internal dissipation holds for a number of known models as well, in particular, for models with fractional exponential kernels, [21]. It gives nontrivial restrictions on the form of constitutive equations of the differential type. As an example we consider the Hohenemser–Prager equation, [22]:

$$a_0\, \sigma + a_1\, \dot{\sigma} = b_0\, \varepsilon + b_1\, \dot{\varepsilon}$$

with constant phenomenological coefficients a_k and b_k. In this case the Fourier transform of the relaxation kernel is as follows

$$\widehat{\varphi}(\omega) = \frac{b_0 + \imath\, \omega\, b_1}{a_0 + \imath\, \omega\, a_1} = \frac{(b_0 + \imath\, \omega\, b_1)(a_0 - \imath\, \omega\, a_1)}{a_0^2 + \omega^2 a_1^2},$$

and the inequality (2.26) results in the condition $a_0\, b_1 \geq a_1\, b_0$.

For the description of rheological properties of materials the Cole–Cole model, [13], with coefficients E_0, E_∞, η, and $\alpha \geq 0$, for which

$$\widehat{\varphi}(\omega) = E_\infty - \frac{E_\infty - E_0}{1 + \left(\imath\, \omega/\omega_\eta\right)^\alpha}, \quad \omega_\eta = \frac{E_\infty - E_0}{\eta},$$

is often used. This is a version of a model with a fractional exponential relaxation kernel. For it Eq. (2.25) holds only if all coefficients are real. From (2.25) for $\omega \to 0$ it follows that $\overline{E}_0 = E_0$. Similarly for $\omega \to \infty$ we have $\overline{E}_\infty = E_\infty$. If $\Im\, \omega_\eta \neq 0$ or $\Im\, \alpha \neq 0$ then the equation is not valid for intermediate values of ω.

To satisfy the inequality (2.26), the difference $E_\infty - E_0$ must be non-negative and the coefficient α may not exceed 2. Indeed, since

$$\imath^{\,\alpha} = e^{\imath \pi \alpha/2} = \cos \frac{\pi \alpha}{2} + \imath \sin \frac{\pi \alpha}{2},$$

the quantity

$$\Im\, \widehat{\varphi}(\omega) = \frac{\left(E_\infty - E_0\right)\left(\omega/\omega_\eta\right)^\alpha}{1 + \left(\omega/\omega_\eta\right)^{2\alpha}}\, \Im\, \imath^{\,\alpha}$$

is non-negative that provides dissipation of a model.

References

1. Badiche, X., Forest, S., Guibert, T., Bienvenu, Y., Bartout, J.D., Ienny, P., Croset, M., Bernet, H.: Mechanical properties and non-homogeneous deformation of open-cell nickel foams: application of the mechanics of cellular solids and of porous materials. Mater. Sci. Eng. A Struct. Mater. Prop. Microstruct. Process. **289** (1–2), 276–288 (2000)
2. Banhart, J., Baumeister, J.: Deformation characteristics of metal foams. J. Mater. Sci. **33** (6), 1431–1440 (1998)
3. Biot, M.A.: Theory of finite deformations of porous solids. Indiana Univ. Math. J. **21**, 597–735 (1972)
4. Biot, M.A.: Nonlinear and semilinear rheology of porous solids. J. Geophys. Res. **78** (23), 4924–4937 (1973)
5. de Boer, R.: Theory of Porous Media: Highlights in the Historical Development and Current State. Springer, New York (1999)
6. Borja, R.I.: Multiscale modeling of pore collapse instability in high-porosity solids. In: Soares, C.A.M., Martins, J.A.C., Rodrigues, H.C. (eds.) Computational Mechanics: Solids, Structures and Coupled Problems, pp. 165–172. Springer, Netherlands (2006)
7. Breuer, S., Onat, E.T.: On uniqueness in linear viscoelasticity. Q. Appl. Math. **19** (4), 355–359 (1962)
8. Bulavskii, V.A.: Metody Relaksaczii dlya Sistem Neravenstv (Relaxation Methods for Systems of Inequalities). Izd. Novosib. Univ., Novosibirsk (1981)

9. Bykovtsev, G.I., Ivlev, D.D.: Teoriya Plastichnosti (Plasticity Theory). Dal'nauka, Vladivostok (1998)
10. Carcione, J.M.: Viscoelastic effective rheologies for modeling wave propagation in porous media. Geophys. Prospect. **46**, 249–270 (1998)
11. Carroll, M.M., Holt, A.C.: Static and dynamic pore-collapse relations for ductile porous materials. J. Appl. Phys. **43**, 1626–1636 (1972)
12. Christensen, R.M.: Theory of Viscoelasticity, 2nd edn. Dover Publications Inc., Mineola (2010)
13. Cole, K.S., Cole, R.H.: Dispersion and absorption in dielectrics—I. Alternating current characteristics. J. Chem. Phys. **9**, 341–351 (1941)
14. Day, W.A.: The Thermodynamics of Simple Materials with Fading Memory, Springer Tracts in Natural Philosophy, vol. 22. Springer, New York (1972)
15. Ehlers, W. (ed.): Theoretical and Numerical Methods in Continuum Mechanics of Porous Materials, Solid Mechanics and Its Applications. IUTAM Symposium. Kluwer Academic Publishers, Netherlands (2001)
16. Gibson, L.J.: Properties and applications of metal foams. In: Kelly, A., Zweben, C. (eds.) Comprehensive Composite Materials, Metal Matrix Composites. vol. 3, pp. 821–842. Pergamon Press, Oxford (2000)
17. Gibson, L.J., Ashby, M.F.: Cellular Solids: Structure and Properties. Cambridge Solid State Science Series. Cambridge University Press, Cambridge (1997)
18. Gnoevoi, A.V., Klimov, D.M., Chesnokov, V.M.: Osnovy Teorii Techenii Bingamovskikh Sred (Foundations of the Theory of Flows of Bingham Media). Fizmatlit, Moscow (2004)
19. Green, R.J.: A plasticity theory for porous solids. Int. J. Mech. Sci. **14**, 215–224 (1972)
20. Nesterenko, V.F.: Dynamics of Heterogeneous Materials. Springer, New York (2001)
21. Rabotnov, Y.N.: Elements of Hereditary Solid Mechanics. Mir Publishers, Moscow (1980)
22. Reiner, M.: Deformation, Strain and Flow: an Elementary Introduction to Rheology. H. K. Lewis, London (1960)
23. Rockafellar, R.T.: Convex Analysis. Princeton University Press, Princeton (1970)
24. Sadovskaya, O.V., Sadovskii, V.M.: Rheological models of uniaxial deformation of porous media. Vestnik Krasnoyarsk. Univ.: Fiz.-Mat. Nauki **9**, 202–206 (2006)
25. Sadovskaya, O.V., Sadovskii, V.M.: Models of rheologically compicated media with different resistances to tension and compression. In: Mathematical Models and Methods of Continuum Mechanics: Collected Papers, pp. 224–238. IAPU DVO RAN, Vladivostok (2007)
26. Sadovskii, V.M.: Numerical modeling in problems of the dynamics of granular media. In: Proceedings of the Mathematical Centre N. I. Lobachevskii, Izd. Kazansk. Mat. Obshhestva, Kazan, vol. 15, pp. 183–198 (2002)
27. Sadovskii, V.M.: To the theory of elastic-plastic waves propagation in granular materials. Doklady Phys. **47** (10), 747–749 (2002)
28. Sadovskii, V.M.: Rheological models of hetero-modular and granular media. Dal'nevost. Mat. Zh. **4** (2), 252–263 (2003)
29. Sevostianov, I., Kachanov, M.: On the yield condition for anisotropic porous materials. Mater. Sci. Eng. A **313** (1–2), 1–15 (2001)
30. Vinogradov, G.V., Malkin, A.Y.: Rheology of Polymers. Springer, New York (1980)
31. Zintchenko, V.A., Sadovskaya, O.V., Sadovskii, V.M.: A numerical algorithm and a computer system for the analysis of rheological schemes. Numer. Methods Program. Adv. Computing **7** (2), 125–132 (2006)